Renaissance of the ∼1 TeV fixed-target Program

Names

Abstract: This document describes the physics potential of a new Fixed-Target program based on a ∼1 TeV proton source. Two proton sources are potentially available in the future: the existing Tevatron at Fermilab, which can provide 800 GeV protons for fixed-target physics, and a possible upgrade to the SPS at CERN, called SPS+, which would produce 1 TeV protons on target. In this paper we use an example Tevatron Fixed-Target Program to illustrate the high discovery potential possible in the charm and neutrino sectors. We highlight examples which are either unique to the program or difficult to accomplish at other venues.

1 Introduction

Fixed-target at approximately TeV energies? Didn't we do that for over twenty years ending a decade ago? Why revisit that strategy?

A renaissance in TeV-energy fixed-target physics has become possible because of new detector technologies and improvements in accelerators since the 1990's. As a result, we can describe a fixed-target physics program, focusing on the charm and neutrino sectors. The program is unique to a ∼1 TeV fixed-target facility and complements the ongoing physics program envisioned by the community for the late 2010's.

There are two possible sources of ∼1 TeV protons which may be available. The first is the Tevatron at Fermilab, which can be modified for fixed-target running. Details on how this machine can be run at higher intensity and higher efficiency than in the past are discussed in Appendix A of this paper. The second possible source is the SPS+ which is planned at CERN as part of the LHC upgrade program. The fixed-target program described here can run during times when the SPS+ is not providing beam to LHC. The energy of SPS+ is expected to be about 1 TeV. For the results presented here, we have assumed 800 GeV protons on target since this is the capability of the existing machine. However, the physics case only improves for running at 1 TeV.

The purpose of this paper is to illustrate the strength and richness of this fixed-target program. In particular, this paper concentrates on a new study of discovery potential in the charm sector, which would utilize slow-spill beams. A future D^0-$\overline{D}^0$ mixing and CP violation (CPV) experiment with three years of running could reconstruct an order of magnitude more flavor-tagged $D^0 \to K^+\pi^-$ decays than will be reconstructed by the B-factory experiments with their full data sets. The resulting sensitivity to CPV parameters $|q/p|$ and $\mathrm{Arg}(q/p)$ is found to be much greater than current world sensitivity. However, to illustrate that this is a well-rounded program, we also explore ideas in the neutrino sector. We review the case for a precision electroweak neutrino experiment running from a very pure sign-selected high energy ν_μ beam, which has been discussed in more detail elsewhere [**?**, **?**] and we present new studies on two promising and unique avenues for beyond Standard Model neutrino searches using beam dump production. The first of these uses ν_τ charged current events produced by a proton beam in the 800 GeV to 1 TeV range. The second is a search for neutral heavy leptons produced in the beam dump.

This combination of experiments represents an integrated program aimed at discovery of new physics. At the same time, each of these experiments also will provide a wide array of interesting and valuable measurements within the Standard Model. The program is very physicsrich and will provide

opportunities for many physicists. The result is a compelling opportunity for the future.

2 The Discovery Potential of fixed-target Charm

2.1 INTRODUCTION

As mentioned, there was a very successful fixed-target charm program at the Fermilab Tevatron [1]. Not only did it provide high precision measurements (some of which remain the most precise even today), but it also advanced flavor physics thinking in a way that still underlies many current analyses. It also demonstrated the utility of precision vertexing for heavy flavor physics, paving the way for the incorporation of silicon tracking systems in all the latest experiments. The fixed-target charm program ended when the technologies used were more-or-less played out, and attention turned to the opportunities at colliders, both at e^+e^- and hadron machines. The reason to now revisit the possibility of a fixed-target charm experiment is a combination of increased interest in charm mixing (now observed) and possible CPV in the charm system, and the availability of technology well beyond what was available at the end of the previous program. A Tevatron fixed-target experiment may be the most cost-effective way forward in the charm sector, as the Tevatron would not need to be run in collider mode. Also, the beam energy could be reduced and still remain far above charm production threshold. Such an experiment at the Tevatron has the potential to greatly improve upon the sensitivity to mixing and CPV achieved by the B factories. We note that the most sensitive measurements of mixing and CPV rely on measuring decay-time distributions. For this type of measurement, a fixed-target experiment has an advantage over an e^+e^- B factory experiment due to the fact that the mean decay length is notably larger than the vertex resolution. We will address these physics opportunities below. In the recent "Roadmap for US High-Energy Physics" written by the Particle Physics Project Prioritization Panel (P5), future operation of the Tevatron was not considered. However, there exists a plan to keep the Tevatron cold after completion of the collider program such that it could easily be operated again should sufficiently compelling physics opportunities arise.

A Fermilab Tevatron fixed-target experiment could produce very large samples of D^* mesons that decay via $D^{*+} \to D^0\pi^+$, $D^0 \to K^+\pi^-$ [2]. The decay time distribution of the "wrong-sign" $D^0 \to K^+\pi^-$ decay is sensitive to D^0-$\overline{D}^0$ mixing parameters x and y. Additionally, comparing the D^0 decay time distribution to that for $\overline{D}^0$ allows one to measure or constrain the CPV parameters $|q/p|$ and $\mathrm{Arg}(q/p) \equiv \phi$. This method has been used previously by Fermilab experiments E791 [3] and E831 [4] to search for D^0-$\overline{D}^0$ mixing. However, those experiments ran in the 1990's and reconstructed only a few hundred flavor-tagged $D^0 \to K^+\pi^-$ decays. Technological advances in vertexing detectors and electronics made since E791 and E831 ran now make a much improved fixed-target experiment possible. We estimate the expected sensitivity of such an experiment, and compare it to that of the B factory experiments Belle and BaBar. Those experiments have reconstructed several thousand signal decays and, using these samples along with those for $D^0 \to K^+K^-/\pi^+\pi^-$, have made the first observation of D^0-$\overline{D}^0$ mixing [5, 6]. The CDF experiment has also measured D^0-$\overline{D}^0$ mixing using $D^0 \to K^+\pi^-$ decays [7]. Although the background is much higher than at an e^+e^- experiment, the number of reconstructed signal decays is larger, and the statistical errors on the mixing parameters are similar to those of BaBar.

Although we focus on measuring x, y, $|q/p|$, and ϕ, a much broader charm physics program is possible at a Tevatron experiment. We also briefly present some of these other opportunities.

2.2 EXPECTED SIGNAL YIELD

We estimate the signal yield expected by scaling from two previous fixed-target experiments, E791 at Fermilab and *HERA-B* at DESY. These experiments had center-of-mass energies and detector geometries similar to those that a new charm experiment at the Tevatron would have.

2.2.1 Scaling from *HERA-B*

HERA-B took data with various trigger configurations. One configuration used a minimum bias trigger, and from this data set the experiment reconstructed 61.3 ± 13 D^*-tagged "right-sign" $D^0 \to K^-\pi^+$ decays in 182×10^6 hadronic interactions [8]. This yield was obtained after all selection requirements were applied. Multiplying this rate by the ratio of doubly-Cabibbo-suppressed to Cabibbo-favored decays $R_D \equiv \Gamma(D^0 \to K^+\pi^-)/\Gamma(D^0 \to K^-\pi^+) = 0.380\%$ [9] gives a rate of reconstructed, tagged $D^0 \to K^+\pi^-$ decays per hadronic interaction of 1.3×10^{-9}. To estimate the sample size a Tevatron experiment would reconstruct, we assume the experiment could achieve a similar fractional rate. If the experiment ran at an interaction rate of 7 MHz (which was achieved by *HERA-B* using a two-track trigger configuration), and took data for 1.4×10^7 live seconds per year, then it would nominally reconstruct $(7\text{ MHz})(1.4 \times 10^7)(1.3 \times 10^{-9})(0.5) = 64000$ flavor-tagged $D^0 \to K^+\pi^-$ decays per year, or 192000 decays in three years of running. Here we have assumed a trigger efficiency of 50% relative to that of *HERA-B*, as the trigger would need to be more restrictive than the minimum bias configuration of *HERA-B*.

2.2.2 Scaling from E791

Fermilab E791 was a charm hadroproduction experiment that took data during the 1991-1992 fixed-target run. The experiment ran with a modest transverse-energy threshold trigger, and it reconstructed 35 D^*-tagged $D^0 \to K^+\pi^-$ decays in 5×10^{10} hadronic interactions [3]. This corresponds to a rate of 7×10^{-10} reconstructed decays per hadronic interaction. Assuming a future Tevatron experiment achieves this fractional rate, one estimates a signal yield of $(7\text{ MHz})(1.4 \times 10^7)(7 \times 10^{-10}) = 69000$ per year, or 207000 in three years. This value is similar to that obtained by scaling from *HERA-B*. We have assumed the same trigger + reconstruction efficiency as that of E791. We note that E791 had an inactive region in the middle of the tracking stations where the π^- beam passed through, and a future Tevatron experiment could avoid this acceptance loss. We do not include any improvement for this in our projection.

2.3 COMPARISON WITH THE *B* FACTORIES

We compare these yields with those that will be attained by the B factory experiments after they have analyzed all their data. The Belle experiment reconstructed 4024 D^*-tagged $D^0 \to K^+\pi^-$ decays in 400 fb^{-1} of data [10], and it is expected to record a total of 1000 fb^{-1} when it completes running. This integrated luminosity corresponds to 10060 signal events.

The BaBar experiment reconstructed 4030 tagged $D^0 \to K^+\pi^-$ decays in 384 fb^{-1} of data [5], and the experiment recorded a total of 484 fb^{-1} when it completed running in early 2008. Thus the total BaBar data set corresponds to 5080 signal events. Adding this to the estimated final yield from Belle gives a total of 15100 $D^0 \to K^+\pi^-$ decays. This is less than 8% of the yield estimated for a Tevatron experiment in three years of running.

The KEK-B accelerator where Belle runs is scheduled to be upgraded to a "Super-B" factory running at a luminosity of $\sim 8 \times 10^{35}$ cm^{-2} s^{-1} [11]. There is also a proposal to construct a Super-B factory in Italy near the I.N.F.N. Frascati laboratory [12]. An experiment at either of these facilities would reconstruct very large samples of $D^{*+} \to D^0\pi^+$, $D^0 \to K^+\pi^-$ decays. In fact the resulting

sensitivity to x'^2 and y' may be dominated by systematic uncertainties. This merits further study. We note that the systematic errors obtained at a future Tevatron experiment are expected to be smaller than those at an e^+e^- collider experiment, due to the superior vertex resolution and π/K identification possible with a forward-geometry detector.

2.4 COMPARISON WITH HADRON COLLIDERS

The LHCb experiment has a forward geometry and is expected to reconstruct $D^{*+} \to D^0\pi^+$, $D^0 \to K^+\pi^-$ decays in which the D^* originates from a B decay. The resulting sensitivity to mixing parameters x'^2 and y' has been studied in Ref. [13]. This study assumes a $b\bar{b}$ cross section of 500 μb and estimates several unknown trigger and reconstruction efficiencies. It concludes that approximately 58000 signal decays would be reconstructed in 2 fb^{-1} of data, which corresponds to one year of running. This yield is similar to that estimated for a Tevatron experiment. However, LHCb's trigger is efficient only for D mesons having high p_T, *i.e.*, those produced from B decays. This introduces two complications:

1. Some fraction of prompt $\overline{D}{}^0 \to K^+\pi^-$ decays will be mis-reconstructed or undergo multiple scattering and, after being paired with a random soft pion, will end up in the $D^0 \to K^+\pi^-$ sample (fitted for x'^2 and y'). As the production rate of prompt D's is two orders of magnitude larger than that of B's, this component may be non-negligible, and thus would need to be well-understood when fitting.

2. To obtain the D^* vertex position (*i.e.*, the origin point of the D^0), the experiment must reconstruct a $B \to D^*X$ vertex, and the efficiency for this is not known. Monte Carlo studies indicate it is 51% [13], but there is uncertainty in this value.

The LHCb study found that, for $N_{K^+\pi^-} = 232500$, a signal-to-background ratio (S/B) of 0.40, and a decay time resolution (σ_t) of 75 ps, the statistical errors obtained for x'^2 and y' were 6.4×10^{-5} and 0.87×10^{-3}, respectively. These values are less than half of those that we estimate can be attained by the B factories by scaling current errors by $\sqrt{N_{K^+\pi^-}}$: $\delta x'^2 \approx 14 \times 10^{-5}$ and $\delta y' \approx 2.2 \times 10^{-3}$. As the signal yield, S/B, and σ_t of a future Tevatron experiment are similar to those for LHCb, we expect that similar errors for x'^2 and y' can be attained.

The CDF measurement of charm mixing [7] has 12700 $D^{*+} \to D^0\pi^+$, $D^0 \to K^+\pi^-$ decays from 1.5 fb^{-1} of integrated luminosity. This could increase by about a factor of five by the end of Run II at the Tevatron collider.

To compare to these estimates, we have done a "toy" Monte Carlo (MC) study to estimate the sensitivity of a Tevatron experiment. The results obtained are similar to those of LHCb: for $N_{K^+\pi^-} = 200000$, $S/B = 0.40$, $\sigma_t = 75$ ps, and a minimum decay time cut of $0.5 \times \tau_D$ (to reduce combinatorial background), we find $\delta x'^2 = 5.8 \times 10^{-5}$ and $\delta y' = 1.0 \times 10^{-3}$. These errors are the RMS's of the distributions of residuals obtained from fitting an ensemble of 200 experiments. A typical fit is shown in Fig. 1.

2.5 GLOBAL FIT FOR *CPV* PARAMETERS

If we assume the $\delta x'^2$ and $\delta y'$ errors obtained in our toy MC study (which are close to the values obtained in the LHCb study), we can estimate the resulting sensitivity to CPV parameters $|q/p|$ and ϕ. The first parameter characterizes CPV in the mixing of D^0 and $\overline{D}{}^0$ mesons, while the second parameter is a phase that characterizes CPV resulting from interference between an amplitude with mixing and a direct decay amplitude. In the Standard Model, $|q/p|$ and ϕ are essentially 1 and 0, respectively; a measurable deviation from these values would indicate new physics.

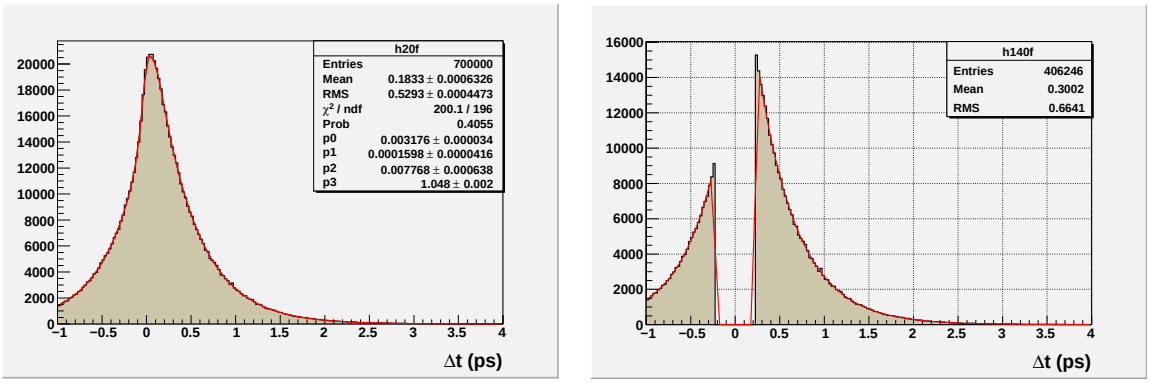

Figure 1: Monte Carlo $D^0 \to K^+\pi^-$ decay time distributions (left) without and (right) with a minimum decay time cut. Superimposed is the result of a fit. The ratio of signal to background after the $t_{\rm min}$ $(=\tau_D/2)$ cut is 0.40, and the decay time resolution σ_t is 75 fs.

To calculate the sensitivity to $|q/p|$ and ϕ, we do a global fit of eight underlying parameters to 28 measured observables. The fitted parameters are x and y, strong phases $\delta_{K\pi}$ and $\delta_{K\pi\pi}$, R_D, and CPV parameters A_D, $|q/p|$ and ϕ. Our fit is analogous to that done by the Heavy Flavor Averaging Group (HFAG) [14]. The only difference is that we reduce the errors for x'^2 and y' according to our toy MC study, and we also reduce the error for y_{CP} by a similar fraction. This latter parameter is measured by fitting the decay time distribution of $D^0 \to K^+K^-/\pi^+\pi^-$ decays, which would also be triggered on and reconstructed by a Tevatron charm experiment.

The results of the fit are plotted in Fig. 2b. The figure shows two-dimensional likelihood contours for $|q/p|$ and ϕ; for comparison, the analogous HFAG plot is shown in Fig. 2a. One sees that a future Tevatron experiment would yield a very substantial improvement.

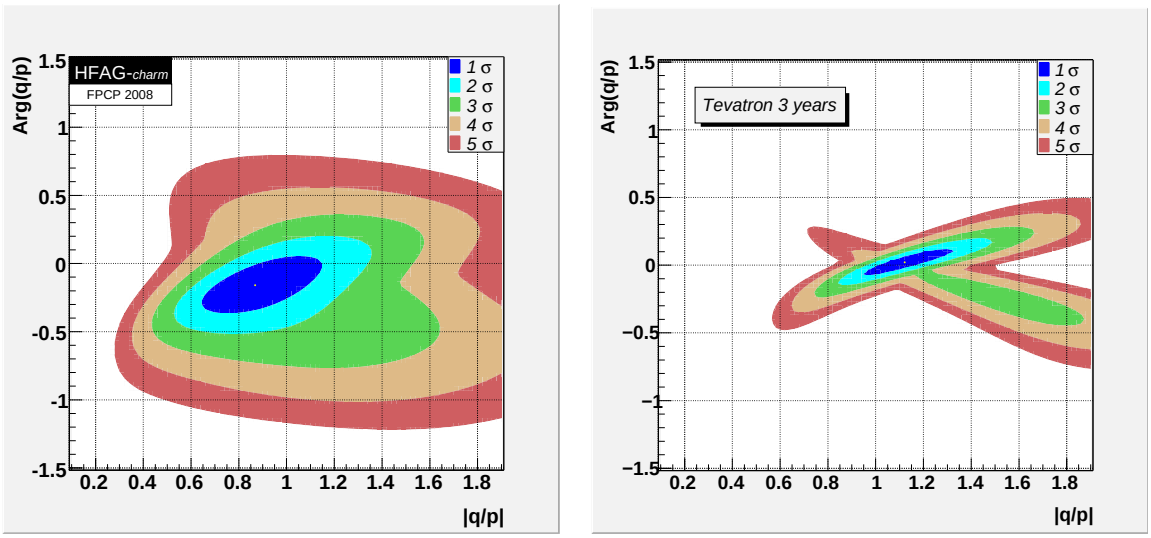

Figure 2: $|q/p|$ versus ϕ likelihood contours resulting from a global fit to measured observables (see text). Left: data after FPCP 2008, from the HFAG [14]. Right: after three years of running of a Tevatron charm experiment.

Table 1: CP asymmetry $A_{CP} = [\Gamma(D^+) - \Gamma(D^-)]/[\Gamma(D^+) + \Gamma(D^-)]$ for $D^\pm$ decays.

Mode	**Year**	**Collaboration**	$\boldsymbol{A_{CP}}$
$\boldsymbol{D^+ \to K^0_s \pi^+}$	2007	CLEOc [27]	$-0.006 \pm 0.010 \pm 0.003$
	2002	FOCUS [33]	$-0.016 \pm 0.015 \pm 0.009$
$\boldsymbol{D^+ \to K^0_s K^+}$	2002	FOCUS [33]	$+0.071 \pm 0.061 \pm 0.012$
$\boldsymbol{D^+ \to \pi^+\pi^-\pi^+}$	1997	E791 [34]	-0.017 ± 0.042 (stat.)
$\boldsymbol{D^+ \to K^-\pi^+\pi^+}$	2007	CLEOc [27]	$-0.005 \pm 0.004 \pm 0.009$
$\boldsymbol{D^+ \to K^0_s \pi^+ \pi^0}$	2007	CLEO-c [27]	$+0.003 \pm 0.009 \pm 0.003$
$\boldsymbol{D^+ \to K^+K^-\pi^+}$	2007	CLEO-c [27]	$-0.001 \pm 0.015 \pm 0.008$
	2005	BABAR [35]	$+0.014 \pm 0.010 \pm 0.008$
	2000	FOCUS [19]	$+0.006 \pm 0.011 \pm 0.005$
	1997	E791 [34]	-0.014 ± 0.029 (stat.)
	1994	E687 [22]	-0.031 ± 0.068 (stat.)
$\boldsymbol{D^+ \to K^-\pi^+\pi^+\pi^0}$	2007	CLEOc [27]	$+0.010 \pm 0.009 \pm 0.009$
$\boldsymbol{D^+ \to K^0_s \pi^+\pi^+\pi^-}$	2007	CLEOc [27]	$+0.001 \pm 0.011 \pm 0.006$
$\boldsymbol{D^+ \to K^0_s K^+\pi^+\pi^-}$	2005	FOCUS [32]	$-0.042 \pm 0.064 \pm 0.022$

2.6 OTHER PHYSICS

2.6.1 Direct CPV searches

In addition to searching for CPV arising from D^0-$\overline{D}^0$ mixing, one can search for direct CPV i.e. CP violation occurring in the decay amplitudes themselves. To search for this, one uses tagged D^+ or D^0 decays and looks for an asymmetry between the $D \to f$ and $\overline{D} \to \bar{f}$ decay rates.

Tables 1-2 are from the HFAG [15] and list current measurements of numerous direct CPV decay modes. Modes with 2- and 3-body final states could potentially be triggered on in a fixed-target Tevatron experiment and thus could be studied. The sensitivity to many of these modes may be substantially greater than that of the current generation of experiments.

2.6.2 Rare and forbidden charm decays

2.6.3 Spectroscopy via Dalitz-plot analyses

A very high statistics charm experiment can hope to unravel many mysteries related to resonances in the 1-2 GeV region. This is because charm hadron masses are in the 2 GeV range and $\pi\pi$, $K\pi$ and KK resonances often dominate charm particle decays. For instance, one can aspire to improve many aspects of our understanding as outlined below. There is much to be learned also from the decays of the $J/\psi, \psi(2S)$, and even the η_c, which could also be produced at some level in any such experiment.

Model-independent scattering amplitudes Investigators such as Dunwoodie, Meadows *et al.* have pioneered the approach of not parameterizing the scattering amplitude but, instead, obtaining amplitudes and phases as a function of energy directly from the data. This gets around many of the problems that plague the various parameterizations. On the other hand, it is not easy to obtain convergent fits to data when a complex amplitude is desired in fine steps of mass. Current results with this technique are in good agreement with the simple isobar model. The true benefits will

Table 2: CP asymmetry $A_{CP} = [\Gamma(D^0) - \Gamma(\overline{D}{}^0)]/[\Gamma(D^0) + \Gamma(\overline{D}{}^0)]$ for $D^0, \overline{D}{}^0$ decays.

Mode	**Year**	**Collaboration**	$\boldsymbol{A_{CP}}$
$\boldsymbol{D^0 \to \pi^+\pi^-}$	2008	BABAR [17]	$-0.0024 \pm 0.0052 \pm 0.0022$
	2005	CDF [18]	$+0.010 \pm 0.013 \pm 0.006$
	2002	CLEO [16]	$+0.019 \pm 0.032 \pm 0.008$
	2000	FOCUS [19]	$+0.048 \pm 0.039 \pm 0.025$
	1998	E791 [20]	$-0.049 \pm 0.078 \pm 0.030$
$\boldsymbol{D^0 \to \pi^0\pi^0}$	2001	CLEO [23]	$+0.001 \pm 0.048$ (stat. and syst. combined)
$\boldsymbol{D^0 \to K^0_s\pi^0}$	2001	CLEO [23]	$+0.001 \pm 0.013$ (stat. and syst. combined)
$\boldsymbol{D^0 \to K^+K^-}$	2008	BABAR [17]	$+0.0000 \pm 0.0034 \pm 0.0013$
	2005	CDF [18]	$+0.020 \pm 0.012 \pm 0.006$
	2002	CLEO [16]	$+0.000 \pm 0.022 \pm 0.008$
	2000	FOCUS [19]	$-0.001 \pm 0.022 \pm 0.015$
	1998	E791 [20]	$-0.010 \pm 0.049 \pm 0.012$
	1995	CLEO [21]	$+0.080 \pm 0.061$ (stat.)
	1994	E687 [22]	$+0.024 \pm 0.084$ (stat.)
$\boldsymbol{D^0 \to K^0_s K^0_s}$	2001	CLEO [23]	-0.23 ± 0.19 (stat. and syst. combined)
$\boldsymbol{D^0 \to \pi^+\pi^-\pi^0}$	2008	BABAR [24]	$-0.0031 \pm 0.0041 \pm 0.0017$
	2008	Belle [25]	$+0.0043 \pm 0.0130$
	2005	CLEO [26]	$+0.001^{+0.09}_{-0.07} \pm 0.05$
$\boldsymbol{D^0 \to K^+K^-\pi^0}$	2008	BABAR [24]	$0.0100 \pm 0.0167 \pm 0.0025$
$\boldsymbol{D^0 \to K^-\pi^+\pi^0}$	2007	CLEOc [27]	$+0.002 \pm 0.004 \pm 0.008$
	2001	CLEO [28]	-0.031 ± 0.086 (stat.)
$\boldsymbol{D^0 \to K^+\pi^-\pi^0}$	2005	BELLE [29]	-0.006 ± 0.053 (stat.)
	2001	CLEO [30]	$+0.09^{+0.25}_{-0.22}$ (stat.)
$\boldsymbol{D^0 \to K^0_s\pi^+\pi^-}$	2004	CLEO [31]	$-0.009 \pm 0.021^{+0.016}_{-0.057}$
$\boldsymbol{D^0 \to K^+\pi^-\pi^+\pi^-}$	2005	BELLE [29]	-0.018 ± 0.044 (stat.)
$\boldsymbol{D^0 \to K^+K^-\pi^+\pi^-}$	2005	FOCUS [32]	$-0.082 \pm 0.056 \pm .047$

accrue when differences are well established. It should be noted that the idea that intermediate resonances necessarily exist is not universally accepted. Indeed, such doubts motivated Dunwoodie to advocate that we measure scattering amplitudes directly without any assumptions about resonances, and compare with results in other related processes. Higher statistics than currently available will be required.

Improvement in descriptions of the resonances So far we have mostly used a Breit-Wigner functional form to describe resonances, with some modifications for barrier penetration factors etc. However, there is no well-established theory which prescribes a precise form for the propagator for wide resonances. Hence, deviations from the simple forms are to be expected, particularly for describing broad resonances with high statistics. This is already evident in Dalitz fits to, for example, the $D^0 \to K^0_S \pi\pi$. Another example is that Gounaris and Sakurai provided a formula for the case of the well-known wide resonance $\rho(770)$ [36]. Experimentally, one can try to examine scattering amplitudes [37] and one does not find clear Breit-Wigner-shaped peaks. This further delineates the need for high-statistics studies of scattering.

A related issue is that of parameterization via Breit-Wigner peaks or via the K-matrix and P-vector formalisms [38, 39, 40]. The K-matrix method is well motivated, but does it (a) provide a better description of data than a simple sum of resonances and (b) is it merely a different parameterization since there are hidden assumptions in this approach? A well-known success is the Flatte formula for coupled channel descriptions of the $f_0(980)$. This description is being tested (at least) by BaBaranalysis of $D_s \to \pi\pi\pi$ data at the moment.

Another example of uncertainties in physics descriptions lies in the issue of whether the Zemach formalism or the helicity formalism correctly describes decays [41, 42].

Barrier penetration factors modify the resonant propagators. Their derivation is based on simple quantum mechanical models of mesons [43, 44]. There is no reason to expect these expressions to be rigidly true. Indeed, we must search for better descriptions both empirically as well as theoretically, especially when there are higher mass excitations in the same amplitude (*e.g.*, the P-wave extracted from K pi scattering).

Improvements in masses and widths of well-established resonances It is well known that the parameters (and parameterization) of the f0(980) are not well established. Indeed, as a simple scan of the particle data table of light, unflavored mesons will establish, beyond a mass of around 1 GeV, one or more of the mass, width and major branching fractions of most resonances are not well known. This is also true for strange mesons apart from the $K^*(892)$: the $K^*_2(1430)$, the $K^*_3(1780)$ and the $K^*_4(2045)$. Note however that mass and width values must be in context, *i.e.*, may not be identical in all processes, (*e.g.*, there could be effects due to thresholds or to cross-channel interference in Dalitz-plot analyses.

Note that there is also the possibility of learning about light meson systems from charm baryon decay. For example, in Ziegler's thesis study of $\Lambda_c \to \Lambda K^+ \overline{K}^0$ [45], she showed that the Dalitz plot is well-described in terms of a_0 and $\Xi(1690)$ amplitudes only. It would be interesting to look at the $\Lambda_c \to \Lambda \eta \pi^+$ Dalitz plot in order to relate the a_0 to $K^+\overline{K}^0$ and $\eta\pi^+$ amplitudes, assuming that one can obtain adequate statistics on both Λ_c decay modes.

Sorting out poorly established resonances As stated in the PDF reviews of low mass resonances [46, 47], scalar resonances have large widths; there are many in a short mass interval; and there is "competition" from glueballs and multiquark states. In addition there is the experimental problem of distinguishing these from "non-resonant components" in Dalitz analyses.

A list of issues in charm spectroscopy includes:

- Parameters for the well-established: $K_0^*(1430)$.
- The κ: Wide and close to $K\pi$ threshold; difficult to establish. Connections to theoretical work on poles of the T-matrix have not been firm.
- The $a_0(980)$: Being close to the $K\overline{K}$ threshold, it is difficult to establish this without a proper coupled-channel analysis. The broad structure at 1300 MeV: needs further confirmation in existence and isospin assignment.
- $\sigma(600)$: Hard to establish. Broad, must be "distorted by background as required by chiral symmetry", from "crossed channel exchanges" etc. The $\sigma(600)$ plays an important role as the "Higgs boson of strong interactions" in chiral symmetry-breaking models, and supposedly "generates" most of the proton and η' masses.
- $f_0(980)$: Overlaps strongly with the $\sigma(600)$, if such exists. (Leads to a dip in the $\pi\pi$ spectrum at the $K\overline{K}$ threshold.)
- $f_0(1500)$: Mass is fairly well-established, but not precisely so. Whether this resonance is mainly glue is an open question. Note however that the $f_0(1710)$, is seen in J/ψ radiative decay (indicating gg coupling) while the $f_0(1500)$ is not.
- Pseudoscalars: Is there only a single $\eta(1440)$ or are there also $\eta(1405)$ and $\eta(1475)$? The latter two are not firmly established. Similarly, one can ask whether the $\eta(1295)$ is an established resonance. Theorists have questioned the need for this large number of states. At the same time, classification schemes can accommodate these resonances. Do they have large gluonic content?
- 1^{++} isoscalars: Is the $f_1(1420)$ decaying to $K^*\overline{K}$ real? Similarly, an $f_1(1510)$ is reported, and again, this resonance needs to be firmly established.
- What are the masses, widths and couplings of all these resonances? Knowledge of the branching fractions and coupling information will lead to the clearing up of oddities in data analyses, e.g which channels should show which resonances?
- Interpretation: Fitting the scalars into a nonet is a problem. The choice of the ninth member is ambiguous. Are they dominantly multiquark ($qq\bar{q}\bar{q}$) states? Are they glueballs? And how many of the masses and widths are predicted by lattice gauge calculations?

Spectroscopy via production (*e.g.*, double charm baryons) Doubly-Charmed Baryons were discovered at Fermilab in forward hadroproduction with baryon beams. Several states have been reported, each in several decay modes. However, there has been no confirmation of these states from non-baryon-baryon interactions. These states are a new and different window into QCD. Their spectroscopy, lifetimes, and decay schemes are all illuminating.

There are critical experimental issues for a 100-1000+ event experiment. These include:

- High energy baryon beams
- High rate beam and detector
- Excellent tracking, particularly in the vertex region
- Good downstream hyperon reconstruction efficiency for good charmed baryon reconstruction efficiency
- Excellent particle ID

Comparisons with other experiments:

- LHC
- Super B-Factories

2.7 OVERVIEW OF NEW TECHNOLOGIES

2.7.1 Silicon pixel detectors/vertexing

Silicon pixel detectors will play a crucial role in a new high-rate fixed-target charm experiment. Their contributions include pattern recognition in complex event topologies, radiation-hard high-rate capability so that primary beam can go through the detector without compromising performance, and excellent spatial resolution enabling the reconstruction of interaction and decay points from measured charged particle tracks.

Historically, silicon microstrip detectors played an important role in fixed-target charm experiments. When these high precision vertex detectors were introduced in the eighties, they revolutionized the study of heavy flavors. Besides offering high precision tracking and vertex information, they lead to the possibility of high statistics experiments, something that earlier generations of experiments, using bubble chambers or emulsions could not possibly accomplish. In 1985/1986, CCDs were used in a fixed-target charm experiment, the first application of pixel devices in high energy physics. Since then, silicon strip detectors have become major tracking elements in all collider experiments; for the Tevatron, LEP, B-factories, and now the LHC. CCDs were limited to only e^+e^- colliders because of their readout speed. On the other hand, the use of hybridized pixel detectors, in which readout chips were bump-bonded to silicon sensors, have been used in heavy ion experiments at CERN (WA97, NA62) and are now being employed as the vertex detector for ATLAS, CMS, and ALICE. With the development and experience gained over the last decade or so, the hybridized pixel detector technology has matured, and certainly can be an important tool for future fixed-target charm experiments.

Pixel detectors offer excellent three-dimensional information, which leads to much better pattern recognition, avoiding ambiguities and ghost tracks. Its advantages over the two-dimensional information provided by the silicon strip detectors have been demonstrated by both the fixed-target experiments at CERN and also at SLD. With a pixel size of 50 microns by 400 microns, test beam results achieved a resolution of better than 2 microns. The detector noise is about 100 electrons or less. This means such a detector would give a signal-to-noise of better than 200:1. These detectors are also very quiet, and the spurious hits, as observed during the commissioning phase of the LHC experiments, are of order of 10^{-5}. Furthermore, such devices can be self-triggered. All the readout chips used in the LHC experiments have the feature of being data-driven, which means that the chip generates a fast signal when a hit is registered above threshold. ALICE has used this information, and has taken a lot of cosmic ray and first beam data using a pixel-detector trigger.

Pixel detectors, because of their fine segmentation, can also handle very high rate, and handle high radiation dosage. It has all the excellent features that are required in a next generation of charm experiments.

Since 1998, Fermilab has been active in the pixel R&D effort. This has led to the development of the FPIX series of pixel readout chips for the BTeV experiment. When BTeV was cancelled, a group from Los Alamos picked up the design and used the chip, sensor, interconnect, and a lot of the mechanical design to build a couple of forward muon stations for the PHENIX experiment. With small modifications, such a design could be well suited for a new charm experiment at the Tevatron.

2.7.2 Triggering on decay vertices, impact parameters

With the technical advances in detectors and electronics made since the last Fermilab fixed-target experiments it is now possible to build a high-rate trigger system that selects charm events at the lowest trigger level by taking advantage of the key property that differentiates charm particles from other types of particles, namely their characteristic lifetimes. To achieve this, a new experiment would trigger on charm decay vertices by performing track and vertex reconstruction to search for evidence of a particle-decay vertex that is located tens to hundreds of microns away from a primary interaction vertex. In practice, this would be done by reconstructing primary vertices and selecting events that have additional tracks with large impact parameters with respect to the primary vertex. The main advantage of this approach is that it suppresses light-quark background events while retaining high efficiency for charm events at the first stage of triggering by maximizing the trigger acceptance compared to trigger strategies that rely on detecting specific final-state particles, such as muons, or selecting events based on E_T cuts.

A trigger and data acquisition system for a new charm experiment would be able to take advantage of what has been learned from other experiments. While the power of silicon strip detectors for tracking and vertex reconstruction has been demonstrated by numerous experiments, it is the high-resolution three-dimensional tracking capability provided by a pixel vertex detector that permits a straightforward design for triggering on detached vertices at the first stage of a trigger system. A pixel vertex detector together with zero-suppressed readout of the data provide what is needed to perform the pattern recognition, track reconstruction, vertex reconstruction, and impact-parameter calculations that form the basis for detached-vertex trigger. Moreover, the design of the BTeV experiment demonstrated that the trigger and data acquisition system for a detached-vertex trigger should have the following key features:

- field programmable gate arrays (FPGAs) or comparable devices for pattern recognition;
- low-cost memory to buffer event data and allow for relatively long latencies in the first-level trigger;
- commodity off-the-shelf (COTS) networking and processing hardware.

BTeV demonstrated the possible tradeoffs between calculations performed by FPGAs and general-purpose processors. In the BTeV trigger FPGAs performed most of the pattern recognition for pixel data, since FPGAs excel at performing large numbers of rudimentary calculations in parallel. The remaining calculations were performed by general-purpose processors. One of the key features of the BTeV trigger was flexibility in the design that made it possible to move calculations performed in processors into FPGA hardware, thereby improving performance and reducing the cost of trigger hardware. Several FPGA-based algorithms were developed at Fermilab that could also be applied to a new charm experiment. Examples include an FPGA-based track segment finder and a fast "hash sorter" that sorted track-segment data before sending it to a general-purpose processor.

BTeV also demonstrated that advances in electronics make it possible to build a data acquisition system that will buffer event data long enough for a first-level trigger to analyze every interaction and perform complex operations to search for evidence of a detached vertex. The BTeV trigger design included enough memory to buffer data from the entire detector for approximately 800 ms, which was over three orders of magnitude more than the average processing time required by the first-level trigger. In addition to the large event buffer, the BTeV design relied on commodity networking and processing hardware to implement a sophisticated detached-vertex trigger that could be built for a reasonable cost. The key features of this design are being considered by the LHCb Collaboration for their upgrade in the middle of the next decade.

The CDF experiment has been using a decay-vertex trigger at the second level [48] to record large samples of two-body B and D decays. This success demonstrates the feasibility and capability of a heavy-flavor-decay trigger used in a hadroproduction environment.

2.7.3 RICH detectors, π/K separation

The physics goals of a fixed-target charm experiment require good charged particle identification to observe various decay modes of interest. At the Tevatron fixed-target energies, one must be able to separate pions, kaons, and protons with high efficiency over a range of momentum from several GeV up to hundreds of GeV. This can be accomplished by using a Ring Imaging Cherenkov detector (RICH).

From the early days of the OMEGA experiment, over the years, RICH detectors have been built and operated in different environments. They were used in fixed-target experiments at Fermilab (*e.g.* E665, E706, E789, E781), in *HERA-B* at DESY, as well as in e^+e^- collider experiments (DELPHI and SLD). Currently, a RICH detector is used in a hadron collider experiment (LHCb).

The detector performance and cost is determined, to a large extent, by the choice of the photo-detector. In the early days, experiments used gas detectors based on photo-ionizing gas such as TMAE or TEA. Operationally, this has not been easy. On the other hand, the new rounds of experiments tend to use commercial detectors such as PMT (SELEX), MAPMT (HERA-B) and HPD (LHCb) which offer stability, ease of operation, and maintenance at a moderate cost.

We can take the SELEX RICH as an example. The RICH vessel is 10.22 m long, 93 inches in diameter and filled with neon at atmospheric pressure. At the end of the vessel, an array of 16 hexagonal mirrors are mounted on a low-mass panel to form a sphere of 19.8 m in radius. Each mirror is 10 mm thick, made out of low-expansion glass. For the photo-detector, SELEX used 2848 0.5-inch photomultiplier tubes arranged in an array of 89 by 32. Over a running period of 15 months, detector operation was very stable. The ring radius resolution was measured to be 1.56 mm and, on average, 13.6 photons were observed for a $\beta = 1$ particle.

2.7.4 Micro gas tracking detectors, *e.g.*, GEM

Previous generations of fixed-target charm experiments typically used large area gaseous detectors (*e.g.* drift chambers or multiwire gaseous chambers) for charged-particle tracking purposes. In high rate environments, these detectors suffered from inefficiency. In extreme environments, like regions around the incident beam, there was a dead region. For example, in the charm E-791 experiment at Fermilab, there was a large drift-chamber inefficiency ("hole") around the beam line which had to be constantly monitored and corrected in the Monte Carlo acceptance calculations. This also led to significant loss in the overall efficiency of the spectrometer.

Since the early 1990's, there have been substantial advances in micropattern gaseous detectors. These include MSGC (multistrip gaseous chamber), GEM (gaseous electron multiplier), and Micromega devices. Currently, the state-of-the-art is that chambers as large as $40x40$ cm^2 can be built using either GEMs or Micromegas. These type of detectors have been operated reliably in the last generation of high rate fixed-target experiments such as COMPASS.

In a future high-rate heavy-flavor experiment, one can build a set of Micromegas or GEM detectors near the beam region to handle the high rate. Outside this region, the more conventional drift chambers can be used. This will allow operation at high rates with large area coverage.

2.8 SUMMARY

In summary, we note the following and conclude:

- D^0-$\overline{D}^0$ mixing is now established, and attention has turned to the question of whether there is CPV in this system.

- Technical advances in detectors and electronics made since the last Fermilab fixed-target experiments ran would make a new experiment much more sensitive to mixing and CPV effects. Silicon strips and pixels for vertexing are well-developed, and detached-vertex-based trigger concepts and prototypes exist (*e.g. HERA-B*, CDF, BTeV, LHCb).

- Such an experiment would have substantially better sensitivity to mixing and CPV than all Belle and BaBar data together will provide. The Tevatron data should have less background than LHCb data. Systematic uncertainties may also be less than those of any Super-B Factory experiments and LHCb.

- The Tevatron and requisite beamlines are essentially available.

- Such an experiment could help untangle whatever signals for new physics appear at the Tevatron or LHC.

Recently, a working group has formed to study the physics potential of a charm experiment at the Tevatron in more detail. Information about this working group and its results can be obtained at `http://www.nevis.columbia.edu/twiki/bin/ view/FutureTev/WebHome`.

In brief, we write this chapter to keep the possibility of a fixed-target charm experiment at the Tevatron a viable option for Fermilab (and the US HEP program), to be decided upon once there is a clearer picture of available funding, manpower, and feasibility of the current roadmap.

3 Neutrino-electron Scattering

Neutrino-electron scattering ($\nu_\mu + e \rightarrow \nu_\mu + e$) is an ideal process to search for beyond the Standard Model physics at Terascale energies through precision electroweak measurements. The low cross section for this process demands a very high intensity beam. In order to reduce systematics and reach a cross-section precision better than 1%, this process can be normalized to it's charged-current sister, "inverse muon decay" ($\nu_\mu + e \rightarrow \nu_e + \mu$). The threshold for this interaction is 11 GeV. Therefore, the experiment requires a high energy neutrino flux, as can only be provided by a $\sim$1 TeV proton primary beam. Once a high-energy, high-intensity neutrino flux is established, a detector optimized for $\nu - e$ scattering can also be used for precision structure function and QCD measurements and direct searches.

The physics reach of NuSOnG for Beyond the Standard Model Physics is in the 1 to 7 TeV range, depending on the model. The sensitivity to new physics complements the LHC and brings unique new opportunities to the program. The full physics program is discussed in detail elsewhere [**?**, **?**]. In this paper, we provide an experimental overview which illustrates the value of this endeavor.

3.1 The Beam

For this discussion, we will assume a NuSOnG beam design which is the same as that used by the NuTeV experiment, which ran from 1993-1996 at Fermilab [**?**]. We will assume 2×10^{20} high energy (800 GeV to 1 TeV) protons impinge on a beryllium oxide target. The resulting mesons traverse a quadrupole-focused, sign-selected magnetic beamline, hence the design is called a "sign-selected quad triplet" or SSQT. NuSOnG will run with $1.5{\times}10^{20}$ p.o.t. in neutrino mode, and 0.5×10^{20} p.o.t. in antineutrino mode. The result is a beam of very "right sign" purity ($> 98\%$) and low ν_e contamination (2%). The ν_e in the beam is due mainly to K^+ decays which can be well-constrained by the $K^+ \rightarrow \nu_\mu$ flux which populates the high energy range of the neutrino flux. The magnetic bend substantially reduces ν_e from K_L decay which tend to go forward and will thus not be directed at the detector.

3.2 The Detector: Segmented Glass and LAr Options

The baseline design for the NuSOnG detector is a 3.5 kton glass-target design inspired by the design of the Charm II experiment. The detector is broken into four identical subdetectors, each consisting of a $5\text{m} \times 5\text{m} \times xxx\text{m}$ target followed by an **xx** m long muon spectrometer. Breaking the design into four sections assures high acceptance for muons produced in the target calorimeter to reach the toroid. A gap of **xxx** m extends between each detector to allow for a calibration beam to impinge on the target. The total length of the detector is, therefore, 200 m.

The total target is composed of 2500 sheets of glass which are 2.5 cm (0.25 λ_0) thick. This provides an isoscalar target for neutrino-quark interaction studies. Interspersed between the glass sheets are proportional tubes or scintillator planes. The total target mass is six times greater than NuTeV.

The signal processes are: $\nu_\mu + e \rightarrow \nu_\mu + e$ and $\nu_\mu + e \rightarrow \mu + \nu_e$. These must be distinguished from the backgrounds processes of $\nu_e + n \rightarrow e + p$ and $\nu_\mu + n \rightarrow \mu + p$. These processes become background for certain kinematic cases when the proton is not detected. In the initial studies for NuSOnG, which was designed as interleaved one-radiation length glass targets and live detectors, a large systematic error came from the number of background events where the proton was lost in the glass [**?**]. Protons may be lost in the glass because they are produced at relatively wide angles and low energies. Motivated by this, the collaboration has been considering other designs for a target calorimeter.

LArTPC detectors provide a fully-live alternative in which the proton signature in background events is easily identified. Fig. **??** compares a 60 GeV $\nu - e$ neutral current scatter in an LAr detector (Left) to a typical 60 GeV $\nu_e + n$ background event (Right). One can see that a proton track, which is at a large angle relative to the shower, is clearly visible. A 2 kton LArTPC detector is expected to have similar sensitivity to the 3.5 kton glass NuSOnG detector. An LArTPC would require substantially less electronics than the glass detector, and should be proportionately less expensive.

The NuSOnG LArTPC alternative is very similar in design to the technology for the ν_τ physics discussed later in this paper. Therefore, we defer specifics of construction of a large LAr until section **xxx** of this paper. The similarity between an LAr-based NuSOnG and a future ν_τ detector is demonstrative of the synergy within this overall fixed-target program.

3.3 Neutral & Charged Current Processes

Remarkable rates are acquired when the 3.5 kton detector is combined with the high intensity, high energy beam. One expects > 600M ν_μ CC events and > 65M ν_e CC events. This can be compared to past samples of < 20M [**?**, **?**, **?**, **?**, **?**, **?**, **?**, **?**, **?**] and ~ 500k [**?**, **?**, **?**, **?**, **?**, **?**, **?**, **?**, **?**, **?**, **?**, **?**], respectively. With such large data samples, NuSOnG can search for processes which are within the Standard Model, but rare, or Beyond the Standard Model which have not been studied before.

The expected rates for specific event types are given in Table 3. In particular, one should note that the $\nu - e$ scattering sample is 40 times that of previous experiments.

The high event rates for neutrino neutral current scattering provide a remarkable opportunity to probe for new physics through the weak mixing angle, $\sin^2\theta_W$ and the ratio of neutral to charged current couplings, ρ. This physics can be accessed through four modes: $\nu_\mu + e^- \rightarrow \nu_\mu + e^-$, $\bar{\nu}_\mu + e^- \rightarrow \bar{\nu}_\mu + e^-$, $\nu_\mu + q \rightarrow \nu_\mu + q$, and $\bar{\nu}_\mu + q$. There has been a long history of experiments which have exploited precision neutral current quark scattering, but the ultra-high rates for neutrino electron scattering are a new opportunity raised by the high-energy, high-intensity primary beam. A deviation from the Standard Model predictions in both the electron and quark measurements would present a compelling case for new physics.

An essential feature to the NuSOnG $\nu - e$ study is that the NC event rate can be normalized to the CC process, called "inverse muon decay" (IMD), $\nu_\mu + e^- \rightarrow \nu_e + \mu^-$. This process is well understood in the Standard Model due to precision measurement of muon decay [**?**]. Since the data samples are

600M	ν_μ CC Deep Inelastic Scattering
190M	ν_μ NC Deep Inelastic Scattering
75k	ν_μ electron NC elastic scatters (ES)
700k	ν_μ electron CC quasi-elastic scatters (IMD)
33M	$\bar{\nu}_\mu$ CC Deep Inelastic Scattering
12M	$\bar{\nu}_\mu$ NC Deep Inelastic Scattering
7k	$\bar{\nu}_\mu$ electron NC elastic scatters (ES)
0k	$\bar{\nu}_\mu$ electron CC quasi-elastic scatters (WSIMD)

Table 3: Rates for NuSOnG assuming 2×10^{20} protons on target. NC indicates "neutral current"and CC indicates "charged current."

collected with the same beam, target and detector at the same time, the ratio of ES to IMD events cancels many systematic errors while maintaining a strong sensitivity to the physics of interest. Our measurement goal of the ES to IMD ratio is a 0.7% error, adding systematic and statistical errors in quadrature [**?**]. The high sensitivity which we propose arises from the combined high energy and high intensity of the NuSOnG design, leading to event samples more than an order of magnitude larger than past experiments.

Normalizing the ES to the IMD events – which can only occur because of the TeV-scale primary beam – represents a crucial step forward from past ES measurements, which have normalized neutrino-mode ES measurements to antineutrino mode, $\bar{\nu}_\mu + e^- \to \bar{\nu}_\mu + e^-$[**?**, **?**]. In fact, the level of precision expected from NuSOnG cannot be reached in lower energy experiments using antineutrino normalization. The improvement from the NuSOnG method is in both the experimental and the theoretical aspects of the measurement. First, the flux contributing to IMD and νES is identical, whereas neutrino and antineutrino fluxes are never identical and so require corrections. Second, the ratio of νES to $\bar{\nu}$ES cancels sensitivity to beyond Standard Model physics effects from the NC to CC coupling ratio, ρ, which are among the primary physics goals of the NuSOnG measurement. In contrast, there is no such cancellation in the ES to IMD ratio.

3.4 Beyond Standard Model Reach

Elastic neutrino electron scattering is a purely leptonic electroweak process. It can be computed within the Standard Model, with high precision [66] and hence provides a very clean probe of physics beyond the Standard Model. The effect of new, heavy ($M_{\rm new} \gg \sqrt{s}$) degrees of freedom to $\nu_\mu e^- \to \nu_\alpha e^-$, where $\alpha = e, \mu, \tau$ can be parameterized by the effective Lagrangian

$$\mathcal{L}^e_{\rm NSI} = +\frac{\sqrt{2}}{\Lambda^2}\Big[\,\bar{\nu}_\alpha \gamma_\sigma P_L \nu_\mu\,\Big]\Big[\,\cos\theta\,\bar{e}\gamma^\sigma P_L e + \sin\theta\,\bar{e}\gamma^\sigma P_R e\,\Big]\,. \tag{1}$$

New physics, regardless of its origin[1], manifests itself through two coefficients: Λ and θ. Λ is the mass scale associated with the new physics, while $\theta \in [0, 2\pi]$ governs whether the new physics interacts mostly with right-chiral or left-chiral electrons, and also governs whether the new physics contribution interferes constructively or destructively with the Standard Model process (Z-boson t-channel exchange) in the case $\alpha = \mu$.

Fig. 3 depicts NuSOnG's ability to exclude Λ as a function of θ for $\alpha = \mu$ or $\alpha \neq \mu$ assuming its $\nu - e$ elastic scattering data sample is consistent with Standard Model expectations. It also depicts

[1]We are neglecting neutrino currents involving right-handed neutrinos or lepton-number violation. These are expected to be severely suppressed as they are intimately connected to neutrino masses (and, to a lesser extent, charged-lepton masses). Once constraints related to neutrino masses are taken into account, these contributions are well outside the reach of TeV-sensitive new physics searches.

NuSOnG's ability to measure Λ and θ in case a significant discrepancy is observed. For more details see [67]. In the case $\alpha = \mu$, where new physics effects interfere with the Standard Model contribution, NuSOnG is sensitive to $\Lambda \lesssim 4$ TeV while in the $\alpha \neq \mu$ case the NuSOnG is sensitive to $\Lambda \lesssim 1.2$ TeV. The new physics reach of NuSOnG is competitive and also complementary to that of the LHC, where new physics in the neutrino sector is hard to access. The new physics reach of NuSOnG is competitive with other leptonic probes (which involve only charged leptons), including LEP2 **ref**, and precision measurements of Møller scattering **ref**.

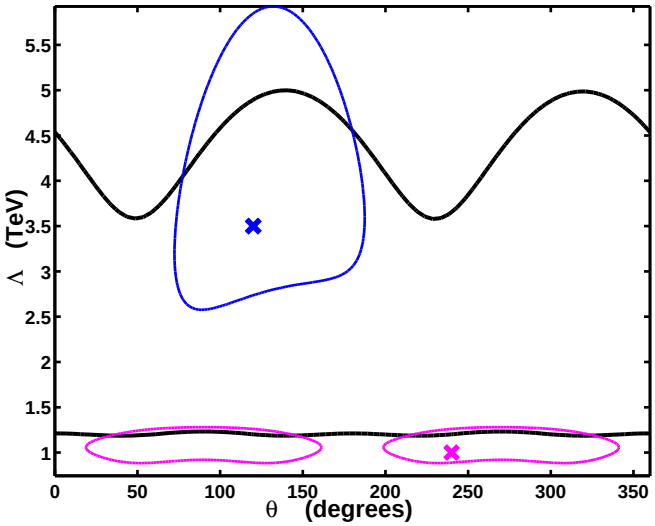

Figure 3: Dark Lines: 95% confidence level sensitivity of NuSOnG to new heavy physics described by Eq. (1) when $\nu_\alpha = \nu_\mu$ (higher curve) and $\nu_\alpha \neq \nu_\mu$ (lower curve). Closed Contours: NuSOnG measurement of Λ and θ, at the 95% level, assuming $\nu_\alpha = \nu_\mu$, $\Lambda = 3.5$ TeV and $\theta = 2\pi/3$ (higher, solid contour) and $\nu_\alpha \neq \nu_\mu$, $\Lambda = 1$ TeV and $\theta = 4\pi/3$ (lower, dashed contour). Note that in the pseudoelastic scattering case ($\nu_\alpha \neq \nu_\mu$) θ and $\pi + \theta$ are physically indistinguishable. From [67].

Several specific new physics scenarios can be probed by a high statistics, high precision measurement of neutrino–matter interactions. NuSOnG's reach to several heavy new physics scenarios is summarized in Fig. 4. There, we consider not only information obtained from neutrino–electron elastic scattering and inverse muon decay but also from neutrino–quark scattering (both neutral current and charge current data). If the new physics scale is below a few TeV, we expect NuSOnG data to significantly deviate from Standard Model expectations. A more detailed comparison of NuSOnG's capabilities is summarized in Table 4.

Table 4: Summary of NuSOnG's contribution in the case of specific models. See [67] for details.

Model	Contribution of NuSOnG Measurement
Typical Z' Choices: $(B - xL)$,$(q - xu)$,$(d + xu)$	At the level of, and complementary to, LEP II bounds.
Extended Higgs Sector	At the level of, and complementary to, τ decay bounds.
R-parity Violating SUSY	Sensitivity to masses ~ 2 TeV at 95% CL. Improves bounds on slepton couplings by $\sim 30\%$ and on some squark couplings by factors of 3-5.
Intergenerational Leptoquarks (non-degenerate masses)	Accesses unique combinations of couplings. Also accesses coupling combinations explored by π decay bounds, at a similar level.

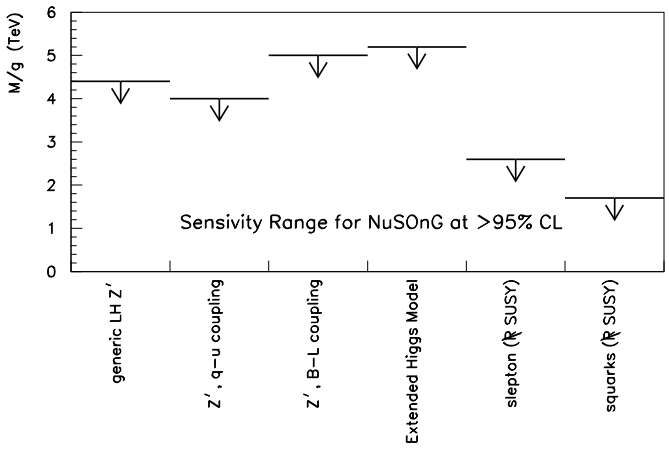

Figure 4: Some examples of NuSOnG's 2σ sensitivity to new high-mass particles commonly considered in the literature. For explanation of these ranges, and further examples, see [67].

Finally, NuSOnG is also sensitive to the existence of new *light* degrees of freedom, including neutral heavy leptons. A particularly interesting signal to look for is wrong-sign inverse muon decay ($\bar{\nu}_\mu + e^- \rightarrow \bar{\nu}_\alpha + \mu^-$), which, given our current understanding of neutrino masses and lepton mixing, only occurs at a negligible level. Wrong-sign inverse muon decay would point to short oscillation length neutrino oscillations mediated by sterile neutrinos, a non-unitary lepton mixing matrix, or other non-standard neutrino interactions.

In summary, NuSOnG is sensitive to a wide range of Beyond Standard Model physics. The program is complementary to new physics which might be observed at LHC. The program is also complementary to the ν_τ experiment and Neutral Heavy Lepton search described below. This unique physics capability arises from the high-flux, high-energy neutrino beam produced by primary protons at $\sim$1 TeV, which allows normalization to IMD events for the first time.

4 ν_τ Experiments

Since the discovery of the charged τ lepton [49], physicists have assumed the existence of a weak partner particle, ν_τ, analogous to the neutrino partners of the e and μ leptons as required by the Standard Model and directly observed for the first time only recently by the DONuT experiment [50, 51]. Indeed, the wealth of studies of charged τ lepton properties also require an accompanying tau-neutrino (ν_τ) for a consistent description of the observed dynamics. Little is directly known about the ν_τ itself.[2] To date, only nine ν_τ charged-current events have ever been detected [50, 51] and all other information

[2]We will henceforth mean by "ν_τ," the neutrino initially prepared in the weak eigenstate with τ lepton number ± 1, as the mass and weak eigenstates of the Standard Model neutrinos have demonstrably been shown to be distinct with the observation of neutrino oscillation.

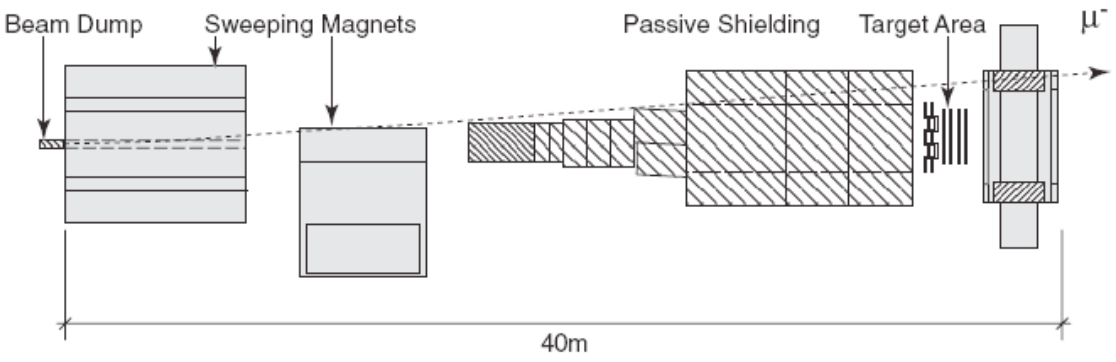

Figure 5: Schematic plan view of the DONuT neutrino beam [50]. The 800 GeV protons are incident on the beam dump from the left. The emulsion modules are located within the target area, 36 m from the beam dump. The trajectory of a 400 GeV/c negative muon is shown. The proposed LArTPC ν_τ observation experiment will be assumed for this discussion to use a similar neutrino production facility with all detector elements downstream of the passive shielding replaced by a LArTPC.

we have on this neutrino weak eigenstate is indirect.[3] An experiment sensitive to τ leptons placed along the path of an intense, ν_τ-rich neutrino beam would add significantly to our understanding of electroweak interactions and would be sensitive to certain hard-to-get manifestations of new physics.

Advances in the development of Liquid Argon Time Projection Chambers (LArTPCs), notably for the ArgoNeuT [55] and MicroBooNE [56] Fermilab projects and ICARUS-T600 [57] at LNGS, suggests it would be a good choice of base detector technology. A 1 kiloton LArTPC would fulfill the physics requirements to discriminate high energy ν_τ charged current interactions while also providing a useful step in the development of LArTPC technology. Experience with progressively larger LArTPC devices will enable easier deployment for future projects with requirements for fiducial masses of 5 kilotons or more, as has been suggested for future long-baseline neutrino-oscillation experiments at the Deep Underground Science and Engineering Laboratory (DUSEL) [58] and other facilities.

4.1 The Neutrino Source

For discussion of this ν_τ experiment, we assume a similar neutrino production facility as was used for DONuT [50], as shown in Fig. 5, but at the higher intensity described elsewhere in this document and using a different detector. Neutrinos delivered to the detector are the result of the decay of particles in hadronic showers produced by primary proton interactions. The primary proton beam is expected to be 800 GeV provided by the FNAL Tevatron or CERN SPS+, in which the maximum center-of-mass energy of an incident proton with a nucleon in the target is approximately 40 GeV, well above threshold to produce charm as well as bottom hadrons. Alternatively, if the primary proton beam were produced by a facility such as CERN's LHC with up to 7 TeV protons in a fixed-target program, the maximum center-of-mass energy rises to approximately 120 GeV, significantly enhancing the ν_τ flux by the decay of produced on-mass-shell Z^0 and $W^\pm$ bosons to charm hadrons, $\tau^\pm$, and ν_τ.

After the interaction of 800 GeV protons with the beam dump, ν_τ are produced primarily by the subsequent decay of produced D_s mesons, with a branching fraction $\mathcal{B}(D_s^- \to \tau^- \bar{\nu}_\tau) = (6.6 \pm 0.6)\%$ [59]. Incident protons are stopped in a beam dump in the form of a tungsten alloy block; DONuT used a 10 cm $\times$ 10 cm $\times$ 1 m water-cooled block. The increased intensity of today's proton facilities may require

[3] Solar and atmospheric neutrino experiments have data which is best interpreted as evidence for ν_τ neutral current interactions. The Super-Kamiokande atmospheric neutrino data also statistically favors the presence of both neutral current and charged current ν_τ initiated events [53, 54].

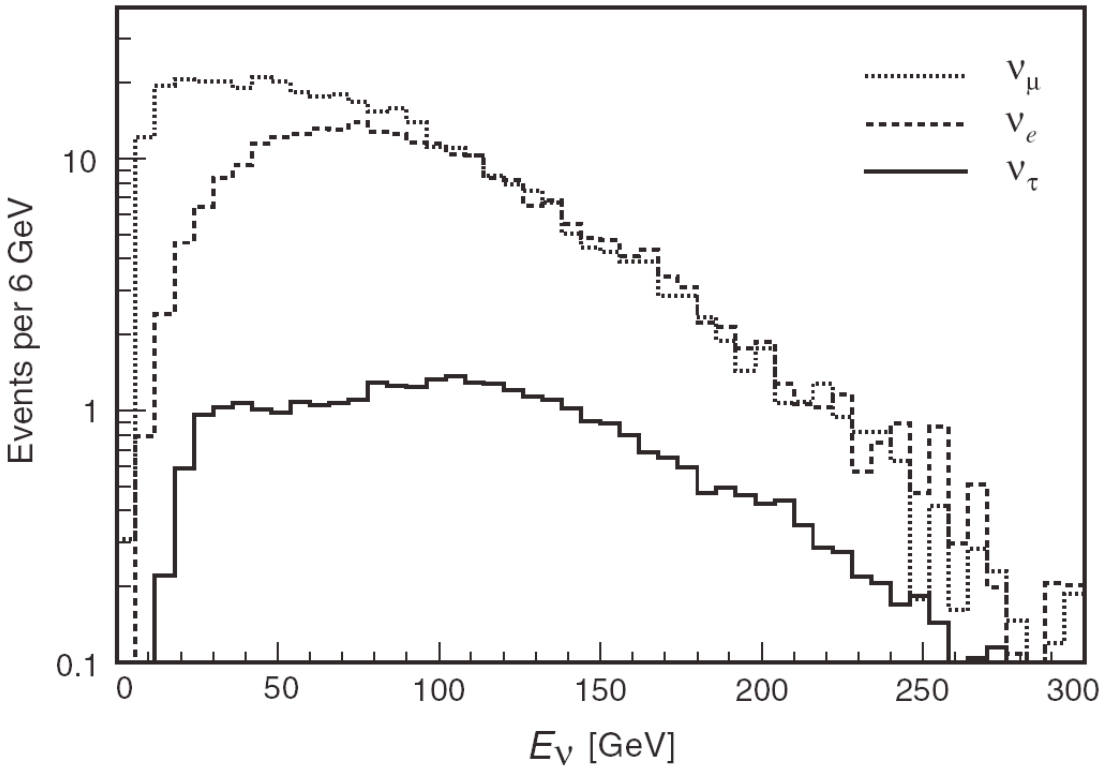

Figure 6: Calculated energy spectra of neutrinos interacting in the DONuT emulsion target [50]. The proposed LArTPC ν_τ observation experiment would see similar spectra at a significantly increased rate.

optimization of the beam dump. Following the beam dump are dipole magnets sufficient to absorb interaction products and deflect away high energy muons from the beam center. After the magnets, a passive absorber is required to further reduce the flux of muons and other interaction products from the beam center. DONuT used 18 m of steel not more than 2 m from the beam center for this purpose. Emerging from this absorber are a reduced flux of muons and a flux of neutrinos of which 3% will be $\nu_\tau + \bar{\nu}_\tau$. The prediction for the spectra of all three neutrino flavors observed at the DONuT emulsion target and using the DONuT beam is shown in Fig. 6. The intensity of the present Tevatron will result in an integrated proton flux approximately 150 times that delivered to DONuT.

4.2 The Detector

The requirements for an optimal neutrino detector include (a) large mass, (b) low unit cost, (c) long-term reliable operation, (d) low energy threshold, (e) high spatial resolution, (f) good energy resolution, (g) homogeneous media allowing consistent detection capability throughout, (h) density and radiation length balanced between event containment and spatial resolution of electromagnetic showers, and (i) high particle-identification efficiency. The DONuT experiment used a primary detector composed of 260 kg of nuclear emulsion modules stacked along the beam line, with each module exposed only for a limited time to avoid track density higher than 10^5 per cm^2. With the increased intensity of the expected proton beam and significantly larger event sample required for a precision ν_τ appearance measurement, an emulsion detector is much more difficult. Technologies that may satisfy the above requirements are water Cherenkov detectors, as employed by (*e.g.*) T2K [60], or LArTPCs used by current and developing experiments ArgoNeuT [55], MicroBooNE [56], and ICARUS-T600 [57].

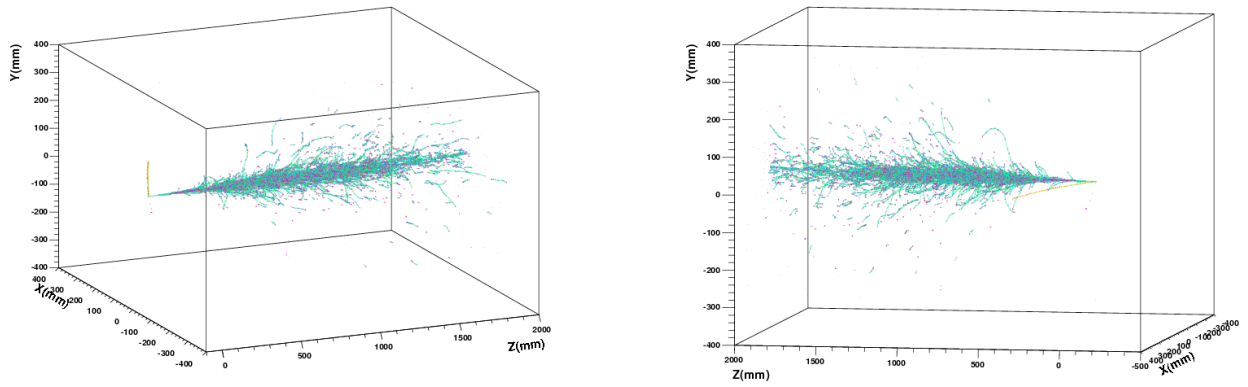

Figure 7: Two arbitrary views of a simulated 193 GeV ν_τ CC interaction in a magnetized MicroBooNE-like LArTPC with 3 mm wire spacing in the charge collection planes. The subsequent 192 GeV τ^- promptly decays as $\tau^- \rightarrow e^- \nu_\tau \bar{\nu_e}$. The proton from a recoil resonance decay ($\Delta^{++} \rightarrow p\ \pi^+$) is also clearly visible. The charge drift direction is along the Y-axis. Assumed single hit position resolution is 3 mm in X and Z, 1.5 mm in Y.

Spatial and energy resolution, low energy threshold, and high-efficiency particleidentificationn are characteristics of LArTPC detectors which will allow the full reconstruction of ν_τ charged-current interactions with efficient identification of the resulting charged τ. The use of a LArTPC as primary detector technology facilitates the identification of typical charged τ decay products with excellent vertex and energy reconstruction sufficient to kinematically reconstruct the intermediate τ. Although ν_τ events can be identified kinematically, it is interesting to note the possibility of reconstructing the short τ track in the highest energy interactions (i.e. a 200 GeV τ travels a mean distance of 9.7 mm, much larger than the position resolution along the beam direction). With this technology, the energy resolution of hits and reconstructed objects within the detector will allow efficient identification of charged particles (electrons, muons, protons, pions, kaons) as well as π^0s, all necessary for kinematic reconstruction of charged τs. Kinematic separation of ν_τ charged current interactions with $\tau \rightarrow \ell\nu\bar{\nu}$ decays from ν_μ and ν_e charged current interactions is possible by analysis of missing transverse momentum, non-zero for ν_τ charged current interactions and close to zero otherwise.

Preliminary scanning of simulated NC and CC ν_e, ν_μ, and ν_τ events up to 300 GeV, based on a MicroBooNE-like LArTPC with 3mm wire spacing, verifies the viability of the technology to meet the physics goals of the proposed experiment. Distinct electromagnetic showers from electrons and photons, tracks from muons, pions, kaons, protons, as well as displaced vertices due to (*e.g.*) photon conversion, K^0_S, and Λ^0, are clearly evident, facilitating the identification of individual particles and resonances. Example simulated ν_τ CC events are shown in Figs. 7 and 8, demonstrating the expected resolution and pattern of energy deposition hits from typical interactions. This position and calorimetric resolution is absolutely necessary in order to kinematically reconstruct a charged τ from its decay products.

The concept of adding a magnetic field to a LArTPC has recently been proposed, with bench tests of its practicality performed on small detectors [61]. This project may offer the first step at deploying the technology at the kiloton scale. If a magnetic field is employed within the TPC, charge-sign identification is possible, which will reduce the combinatorial background in kinematically reconstructing ν_τ charged current interactions, allow separate ν_τ and $\bar{\nu}_\tau$ measurement, provide a method of observing

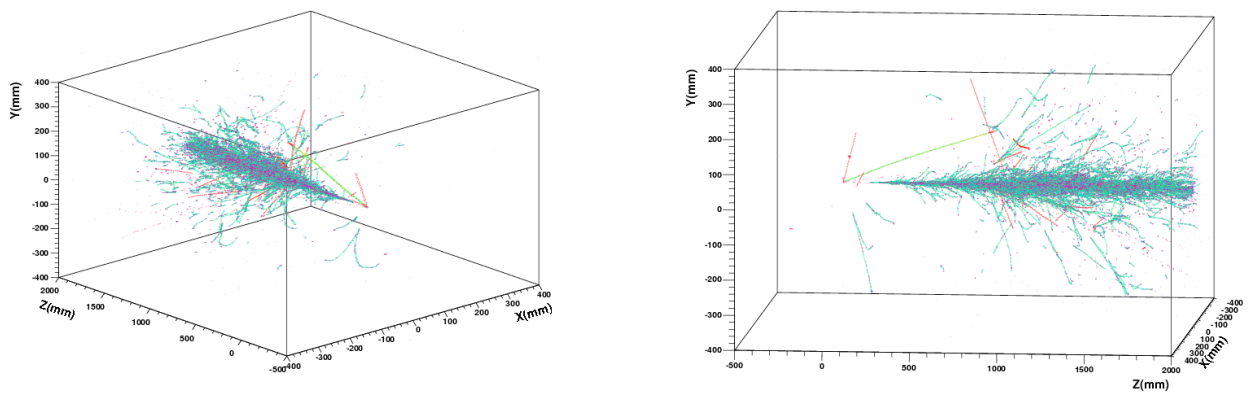

Figure 8: Two arbitrary views of a simulated 220 GeV ν_τ CC interaction in a magnetized MicroBooNE-like LArTPC with 3 mm wire spacing in the charge collection planes. The resulting 212 GeV τ^- decays as $\tau^- \to \rho^- \nu_\tau$. The ρ^- daughter π^- and π^0 yield a clear track and electromagnetic shower emanating from the interaction vertex. The products of a recoil resonance decay ($\Delta^+ \to p\,\pi^0$) are also evident as a low energy vertex proton track and two low energy displaced-vertex daughter photons. The charge drift direction is along the Y-axis. Assumed single hit position resolution is 3 mm in X and Z, 1.5 mm in Y.

potential direct CPV in the neutrino and the charged τ interactions, and provide a second method of track momentum/energy determination especially useful for events with exiting tracks.

One of the major concerns with LArTPC technology is LAr purity, with current technology limiting charge drift distance to less than 2-3 m. The neutrino events at the $\mathcal{O}$(100 GeV) scale will be very forward boosted, such that the LArTPC's drift distance can be short relative to the beam-coordinate. Therefore, sufficient LAr purity may be attained with existing purification technology, even for a kiloton-scale detector, at the expense of additional readout planes or a smaller modular geometry.

Combining the increased flux of protons delivered by the proton source (*e.g.* the FNAL Tevatron), described in the last section, with the use of a LArTPC detector with a mass 2×10^3 times that of DONuT's 0.5 ton as well as twice the running time, will result in a delivered flux observed at the detector approximately 6×10^5 that observed by DONuT over its six-month run, equivalently $\mathcal{O}$(6 million) ν_τ charged current interactions with one year of data.

4.3 The Standard Model and Beyond

Here we highlight the prospects for measuring charged and neutral current ν_τ–matter scattering, observing ν_τ–electron scattering and probing electromagnetic properties of the tau neutrino. In the Standard Model, ν_τ charged current interactions are mediated by W-boson exchange. There is only one measurement (with error bars around 50%) of the charged-current scattering cross-section with initial-state tau neutrinos [50], and it agrees with Standard Model expectations. The expectations are that the $\nu_\tau \to \tau$ transitions are well-described by the Standard Model thanks to abundant data on τ lepton processes, including $\tau \to \nu_\tau \ell \nu_\ell$ ($\ell = e, \mu$), $\tau \to \nu_\tau$+hadrons, $D_{(s)} \to \tau \nu_\tau$, etc. The measurement precision of ν_τ charged-current events is of the utmost importance as it provides a normalization for neutral-current measurements, which are only very poorly constrained. Furthermore, a τ-lepton sensitive neutrino detector may also place bounds on flavor-violating processes such as $\nu_{e,\mu} + X \to \tau + Y$. Even though these are already strongly constrained by the NOMAD experiment [62], a ν_τ-rich beam

might significantly improve on current bounds.

In the Standard Model, neutral current interactions are mediated by Z boson exchange. Unlike charged-current processes, neutral current processes involving ν_τ are only very poorly constrained, especially for interactions with final state ν_τ and ν_e [63]. In more detail, if we add to the Standard Model effective operators of the type (see Eq. (1))

$$\mathcal{L}^{\nu_\tau}_{\rm NSI} = \sum_{f=e,u,d} \frac{\sqrt{2}}{\Lambda^2} \Big[\bar{\nu}_\alpha \gamma_\sigma P_L \nu_\tau \Big] \Big[\cos\theta_f \, \bar{f} \gamma^\sigma P_L f + \sin\theta_f \, \bar{f} \gamma^\sigma P_R f \Big] \,, \tag{2}$$

current data constrain $\Lambda \lesssim 100$ GeV for all f and θ_f for $\alpha = e, \tau$. If present, such weak-scale new physics processes are not only allowed but known to significantly impact the interpretation of neutrino oscillation experiments (see, for example, Ref. [64] for a detailed discussion). A high statistics ν_τ-rich experiment should be able to significantly improve on current bounds or, perhaps, reveal new physics in the neutrino sector.

Finally, a high statistics experiment should also be sensitive to $\nu_\alpha + e$-scattering events. These can be used (see section on NuSOnG) to look for different manifestations of physics beyond the Standard Model. With a ν_τ-rich beam, one can place bounds on what is usually referred to as the magnetic moment of the tau neutrino. In more detail, one is sensitive to interactions of the type

$$\mathcal{L}_{\rm mag.mom.} = \frac{\lambda^{\alpha\beta}}{\Lambda} \Big[\bar{\nu}_\alpha \sigma^{\rho\sigma} \nu_\beta \Big] F_{\rho\sigma}, \tag{3}$$

where $\alpha, \beta = e, \mu, \tau$ and $F_{\rho\sigma}$ is the electromagnetic field-strength. The nature of the dimensionless coefficients λ depends on the nature of the neutrino fields (Majorana versus Dirac) and their magnitude is expected to be negligibly small in the absence of new physics beyond the Standard Model, which here is characterized by the new physics scale Λ. What is referred to as the magnetic moment of a particular neutrino flavor is process dependent and involves different functions of the λ coefficients. While bounds on the ν_e and ν_μ magnetic moments are presently many orders-of-magnitude better than that of ν_τ, it is clear that the information one can acquire with a next-generation ν_τ experiment is independent from and possibly competitive with measurements previous obtained with ν_e and ν_μ scattering (even if neutrinos are Majorana fermions and the appropriate matrix of λ-coefficients is anti-symmetric). The proposed ν_τ experiment is wholly complementary to a next-generation program measuring ν_e and ν_μ scattering, such as NuSOnG. Astrophysics also provides some stringent flavor independent bounds, but these are often model dependent and need to be confirmed by terrestrial experiments. Finally, we note that other electromagnetic properties of the tau neutrino can be probed by neutrino electron scattering (see, for example, Ref. [65]).

Additionally, an intense ν_τ-rich neutrino beam offers a potentially large sample of highly polarized single charged τ leptons which may be uniquely exploited to measure the charged τ anomalous magnetic moment form factor as well as CPV electric dipole moment. This sample of neutrino-produced single τs may also provide an independent measurement of other τ properties in an environment with very different systematic uncertainties than those of the electron-positron collider experiments where the vast majority of τ physics has been studied in the last three decades.

4.4 Primary Measurements

The combination of LArTPC's fast triggering, high spatial and energy resolution, and particle identification by specific ionization energy loss allows a rich program of neutrino physics. The primary measurement of this experiment will be the high precision relative cross section measurement, $\sigma_\tau/\sigma_{(\mu,e)}$, for charged current interactions of ν_e, ν_μ, and ν_τ neutrinos, which provides a sensitive test of the Standard Model as outlined in the previous section. When combined with measurements/limits from NuSOnG

or current limits on the magnetic moment of ν_μ and ν_e, similar searches for events consistent with neutrino magnetic moment interactions in a ν_τ-rich beam can provide sensitivity to the ν_τ magnetic moment comparable to the present limits for ν_e and ν_μ.

Despite the much smaller sample of τs than accumulated by present B-factories ($\mathcal{O}(10^9)$ τs), the unique environment of this detector and production mechanism provide a very different set of systematic uncertainties which allows an interesting laboratory for the verification of virtually all τ properties, including branching fraction measurements as small as $\mathcal{O}(10^{-5})$. For example, utilizing the sample of $\mathcal{O}(10^6)$ charged τ leptons resulting from ν_τ charged current interactions with one year of exposure, several measurements of charged τ properties are also possible. In particular, due to the significant and predictable polarization of the single charged τs produced by ν_τ charged current interactions, this experiment is potentially much more sensitive to the anomalous magnetic moment form factor and electric dipole moment of the charged τ than previous experiments.

Further neutrino physics which may be measurable in this detector includes exclusive cross section measurements, such as coherent-pion production in neutral current and charged current interactions as well as $\nu_\tau e$ charged and neutral current interactions. The significant size and low energy threshold of the LArTPC also allows measurement of solar neutrino rates as well as supernova neutrino sensitivity out of time with the beam spill. The proximity of the detector to the surface, expected pointing resolution of reconstructed tracks, and the size of the detector will yield a significant rate of cosmic-ray induced muons offering a wealth of interesting potential opportunities ranging from the observation of climactic changes in the atmosphere to searching for point sources of cosmic rays and sensitivity to the solar magnetic field.

4.5 ν_τ Summary

Though the ν_τ has been assumed to exist for over thirty years, only nine ν_τ charged current interactions have been observed directly. Precision study of this particle and its interactions is clearly warranted in order to determine if its nature is as predicted by the Standard Model and provides a unique laboratory to search for new physics. The proposed program of neutrino and charged τ physics is broad enough to support a wide variety of studies alongside the primary studies of the electroweak interactions of the ν_τ using $\mathcal{O}(10^5)$ larger sample of interactions than has been observed previously. The proposed 1 kt size of the LArTPC for this experiment is a natural choice to achieve the desired physics goals while also providing an intermediate step in the development of the LArTPC technology between MicroBooNE (100 t) and DUSEL (5+ kt). The addition of a solenoidal field would significantly enhance the physics capabilities of the project while pioneering the technological advancement of coupling LArTPCs with a magnetic field at the kiloton scale.

5 Searches for Exotic Neutrinos

Singlet (sterile) neutrino states arise in models which try to implement massive (light) neutrinos in extensions of the Standard Model. Three singlet states N_1, N_2 and N_3 are associated with the three active neutrinos. In the original see-saw mechanism, these new states have very large masses, but variations like the nMSM model [68] give them masses which are within reach of experimental searches. Limits exist from laboratory experiments, but they extend to masses up to 450 MeV, and apply to couplings with the ν_e or ν_μ. An upgraded Tevatron machine could enlarge the domain of exploration in masses and couplings with the study of neutrinos coming from D and B decays. For the first time, mixings to the ν_τ could be efficiently investigated. Such a search can be envisaged in the beam-dump of the ν_τ experiment.

5.1 Production of sterile neutrinos

If heavy neutrinos exist, they mix with active neutrinos through a unitary transformation. Any neutrino beam will contain a fraction of heavy neutrinos at the level U^2_{Nl} where U denotes the mixing matrix element between the heavy state N and the charged lepton, l (l being e or μ or τ). At low energy accelerators, neutrinos are produced in π and K decays. At higher energies, charm, and beauty contribute. Kinematically, the mass range allowed for the production of a heavy N depends on the emission process. In $\pi \rightarrow \mu + N$ decays, sterile neutrinos can reach a mass of 30 MeV. In $\pi \rightarrow e + N$ channels, the range increases to 130 MeV. Kaons allow larger masses, up to 450 MeV. D decays extend the range to $\sim$1.4 GeV for e and μ channels, (but only to 180 MeV for the τ channel), and B decays to $\sim$4.5 GeV (3 GeV for the τ channel). The flux of N accompanies the flux of known neutrinos at the level of U^2_{Nl}. Corrections to this straightforward result come from helicity conservation which applies differently here. For example, for massless neutrinos, it suppresses $\pi \rightarrow e + \nu$ decays relative to $\pi \rightarrow \mu + \nu$ decays. This is not true anymore for $\pi \rightarrow e + N$. Phase space considerations have also to be taken into account. Thus, precise calculations have to be done in all possible cases to be considered.

5.2 Decays of sterile neutrinos

Ns are not stable. They will decay through purely weak interactions. The lifetime critically depends on the mass considered; it varies as m^5 power. Decay modes also depend on the N mass. As soon as the mass is greater than 1 MeV, the first channel to open is $N \rightarrow ee\nu$. With increasing masses, new modes open, and one can obtain $e\mu\nu$, πe, $\mu\mu\nu$, $\pi\mu$. For higher mass states potentially produced in B decays, new modes become relevant. For example, for masses above 2 GeV, one can envisage the channels De, $D\mu$ or even $D\tau$. Exact branching fractions require precise calculations. The lifetime is given by the formula applying to weak decays, apart from a general suppression factor coming again from the mixing U^2_{Nl}. Other factors coming from helicity and phase space considerations have to be included.

5.3 Previous results

The search consists in looking for a decay signature, typically two charged tracks, one of them being a lepton, and reconstructing a vertex in an empty volume. If no candidates are found, one sets a limit in a two-dimensional plane, mass vs. mixings. Mixings can be equal or different in production and decay. Thus, one tests 6 different combinations of mixings in principle. This has been attempted at CERN by the low energy experiment PS191 [**?**] with 5×10^{18} protons of 19 GeV on target, or about 10^{15} neutrinos (essentially all ν_μ) crossing an empty detector volume. The neutrinos were produced in π and K decays. Thus the limits apply to couplings to ν_e and ν_μ. Kinematically, the τ is not accessible either in production or in decay. The explored mass range is limited to the K mass. The limits on the U^2_{Nl} couplings reach the level of 10^{-8} in a large range of accessible masses and for all combinations of mixings to e or μ. Soon-to-run experiments could improve these results by an order of magnitude. In order to increase the domain of exploration, it is necessary to consider higher energy beams producing neutrinos via D and B decays. D_s decays into $\tau\nu_\tau$, with a branching fraction of 6%. Bs decay into the 3 leptonic channels, $Xe\nu_e$, $X\mu\nu_\mu$, $X\tau\nu_\tau$, with branching fractions 10%, 10% and 5%, respectively. This allows the search of N states with masses up to 4.5 GeV, mixing in particular with the ν_τ. Since the limits vary as the square root of the accumulated neutrino flux, the number of protons on target has to be maximal.

5.4 Detector considerations

The experiment consists in detecting a decay vertex arising in an empty volume set in a neutrino beam and characterized by, in most cases, two charged tracks. The detector requires a decay volume as large as possible followed by a calorimeter. In principle, the search is better done at low energy. However, in order to extend the region of potential masses, one has to produce Bs and this is only done at high energy. The advantage of an upgraded Tevatron machine comes directly from the much increased luminosity available. If, instead of being done in a beam dump, the search is done in a neutrino beam, for example in parallel with NuSOnG, the background coming from neutrino interactions is also substantially increased. In 12 m of air the number of interactions amounts to several 10000 events. Charged current events will give a muon in the final state in 99% of the cases. It becomes essential to have an evacuated volume with a calorimeter to be able to efficiently identify electrons and muons. Studies have been made for the decay volume. A 12 m long pipe where the vacuum can be pushed down to 10^{-3} atm can be seen in Fig. 9. The background from interactions becomes manageable. A higher vacuum would require much more sophisticated techniques. A good spatial resolution plane is necessary between the decay volume and the calorimeter in order to precisely reconstruct the decay vertex. The best limits on couplings come from exclusive channels: πe and $\pi\mu$ for low masses, Ke and $K\mu$ for intermediate masses, and De, $D\mu$, $\pi\tau$ and $D\tau$ for higher masses. The decay channels involving e and μ can be totally reconstructed,. Two essential constraints arise: 1) the reconstructed direction of arrival must point to the neutrino production target and 2) the invariant mass of the detected particles must reconstruct a fixed mass. For example, one can search for a final state $D \to \pi\pi e$. This means that the calorimeter must have the track reconstruction and identification capability. It must be fine grained and preferably come with a magnetic field. These constraints are not applicable for decay modes involving a τ lepton where a characteristic $\pi\tau$ will show up.

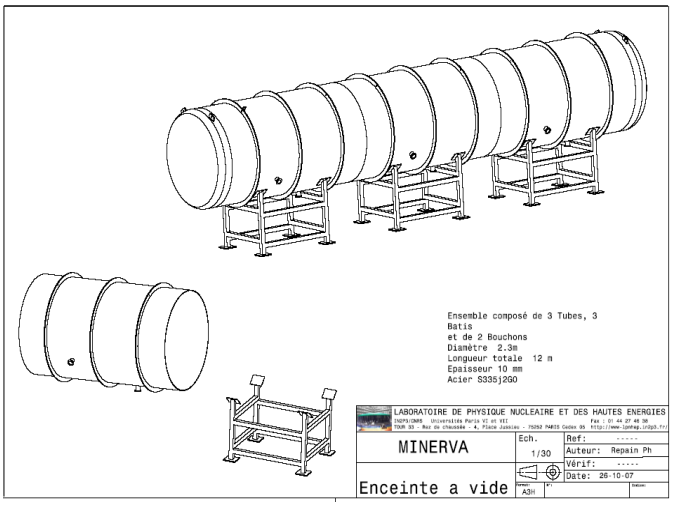

Figure 9: A 12 m long tank for the evacuated decay volume.

5.5 Expectations

Extrapolating the neutrino fluxes used in the ν_τ experiment, one expects about 10^{16} ν_τ per year traversing a 3 m^2 section. Their average energy is 50 GeV. These neutrinos come from D_s decays. Other Ds give about 20 times more ν_e and ν_μ. With a ratio of production cross-sections $B/D \sim 10^{-3}$

one expects of the order of 10^{14} neutrinos of each type coming from Bs. With these numbers, one can estimate the limits obtained by a null experiment in a 10 m long decay volume.

- From D decays one reaches a U^2 limit of 10^{-9} for a mass around 1 GeV and mixings to e and μ.
- From B decays one can reach 10^{-8} for all mixings in particular the never explored $U^2_{\tau\tau}$ around a mass of 3 GeV.

Heavy neutral leptons arise in models which try to accommodate massive active neutrinos. Searches have been done in low energy neutrino beams. The advantage of an upgraded high energy machine is two-fold: the high energy allows exploration in a larger domain of masses, up to the B mass, and the high luminosity pushes down the limits. In particular, it can set meaningful limits on the practically unexplored couplings to the τ. The fascinating possibility of finding sterile neutrinos could be uniquely tested in such an experiment.

6 Conclusions

APPENDIX: Specifics of Running 1 TeV Beams

A The Tevatron

Previous 800 GeV fixed-target operation of the Tevatron ran with a maximum throughput of roughly 25-28 $\times 10^{12}$ protons (25-28 Tp) per pulse every 60 sec with a duty cycle of roughly 33-40%. The beam was shared, over a 20-23 sec flat-top period, between slow spill experiments and neutrino experiments which required fast extracted beams. To meet the demands of NuSOnG, the facility needs to be able to deliver approximately 2×10^{20} protons on target over five years of running at 66% overall operation efficiency per year. This translates to an average particle delivery rate during running of about 1.8 Tp/sec. Assuming that only a 40 second ramp will be required for NuSOnG, each ramping of the Tevatron would need to deliver about 75 Tp, more than 2.5 times the previous record intensity. The subsections below address some of the major issues regarding re-institution of a Tevatron fixed-target program, and issues associated with meeting the above intensity demand.

A.1 Magnet Ramping

The original Tevatron fixed-target program ran at 800 GeV and stress and strain on the superconducting magnets was a major issue early in the program. Issues with lead restraints within the cryostat were eventually identified and all dipole magnets were repaired in the tunnel in the late 1980's. Since that time, the Tevatron has been able to average over 250,000 cycles between failures of dipole magnets [**?**]. This "rate" includes failures of collider-specific magnets, such as low-beta quadrupoles. Note that a neutrino program which demands 2×10^{20} POT, using a synchrotron that delivers 75 Tp every cycle, requires about 2.7 million cycles – thus, on the order of 10 failures could be expected during the course of the experiment.

Once the fixed-target operation was halted and only collider operation was foreseen, the capability to repair and rebuild Tevatron magnets was greatly reduced at the laboratory. However, assuming no need for building new magnets from scratch, capabilities still exist to perform repairs and, along with the given inventory of spare Tevatron magnets and corrector packages, a multi-year fixed-target operation consistent with the above is sustainable from this aspect [**?**].

Ramp rate studies of Tevatron dipole magnets have been performed, and rates of 200-300 A/sec can be maintained at 4.6° K without quenching [**?**]. The current power supply system can still perform at this level. To increase reliability, however, some PS system components may need to be upgraded. Additionally, the Tevatron RF system is still capable of running in the fixed-target state, though beam loading effects and appropriate compensation will need to be investigated for the anticipated higher intensity operation. Two Main Injector pulses would be used to fill the Tevatron. At 3 sec per 150 GeV MI cycle, this constitutes a 15% impact on other MI demands.

A.2 Comments on High intensity

The record intensity extracted from the Tevatron in a cycle at 800 GeV was almost 30 Tp, in 1997, though 20-25 Tp was far more typical. At that time, the bunch length during acceleration would shrink to the point where a longitudinal instability at higher energies (∼600 GeV), resulting in aborts and sometimes quenches. This was compensated as well as possible with "bunch spreading" techniques (blowing up the emittance via RF noise sources). Today, the Main Injector is capable of providing greater than 40 Tp per pulse, which could, in principle, fill the Tevatron to 80 Tp. Many improvements to the Tevatron beam impedance have been made during Run II, including, for example, reduction of the Lambertson magnet transverse impedances which were identified as major sources. Additionally, advances in RF techniques/technology and damper systems, *etc.*, may allow, with enough studies and money, much better compensation of these effects, if required. This is a primary R&D point, if intensities near 75 Tp are to be realized in the Tevatron.

A.3 Re-commissioning of Extraction System

Returning the Tevatron to fixed-target operation would require the re-installation of the extraction channel in the A0 straight section from which beam would be transported to the existing Switchyard area and on to the experimental target station. The electrostatic septa were located at the D0 straight section and could straightforwardly be reinstalled in the original configuration. All of this equipment is currently in storage and available for use. The B0 straight section, currently housing the CDF detector, would be replaced with standard long straight section optical components. Thus, the higher heat leak elements presently installed in the B0 and D0 regions would be absent, requiring less demands from the cryogenics system.

The other necessary piece of hardware is the slow-spill feedback system, referred to as "QXR" which employs fast air-core quadrupoles installed at warm straight sections in the Tevatron for fast feedback tune adjustment during the resonant extraction process. Again, this equipment mostly still exists, though it may be desirable to perform a low-cost upgrade to modernize some electronic components.

The neutrino experiment being discussed has requested "pinged" beam, short bursts of particles brought about by the QXR system. NuSOnG will likely require tens of *pings* per cycle, during an assumed 1 sec flat-top. Resonant extraction is an inherently lossy process, on the scale of 1-2%, determined by the particle step size across the thin electrostatic septum wires. Historically, loss rates were tolerable with between 20-30 Tp extracted over 20 seconds. Extracting 2.5 times this amount in 1/20-*th* the amount of time without quenching the Tevatron will need further study, though should be feasible. Alternative methods for fast extraction could be contemplated, though perhaps at a price. For instance, if an appropriate RF bunching scheme (using a 2.5 MHz RF system, for example) can be employed to prepare bunches spaced by 400 ns, then a fast kicker magnet system might be able to extract 50 such bunches one-by-one to the switchyard, a much cleaner extraction process. Spreading the beam across fewer, longer bunches may also help to mitigate coherent instability issues. This opens up another possible R&D point to pursue. To set the scale, the highest intensity extracted in a single pulse (*i.e.*, not during a slow spill) without quenching the Tevatron was about 10 Tp[**?**]. (Also,

this was a test, not a normal operational procedure.)

The exact method used for 800 GeV operation would be a point closely negotiated between the laboratory and the experiment(s) using the beam. Both resonant extraction and kicker methods should be feasible within reasonable constraints.

A.4 Tevatron abort system

The abort system used during high intensity fixed-target operation was located at C0 and was capable of absorbing 1 TeV proton beams at 30 Tp, repeatedly every "several" seconds, to the abort dump. While not used in collider operation, this beam dump and beam delivery equipment near the C0 straight section is still available and still accessible, and requires re-installation of extraction devices and their power supplies. The ultimate parameters of the neutrino experiment being discussed pushes the beam stored energy from about 3.5 MJ (27 Tp at 800 GeV) toward 10 MJ. The design limits of this system would need to be re-examined, and the implications and environmental impact of re-establishing this area as the primary abort must be looked at carefully.

References

[1] J. A. Appel (Ed.), C. N. Brown (Ed.), P. S. Cooper, H. B. White (Ed.), *Symposium in Celebration of the fixed-target Program with the Tevatron*, FERMILAB-CONF-01-386, hep-ex/0008076 (2000).

[2] Charge-conjugate modes are implicitly included unless noted otherwise.

[3] E. M. Aitala *et al.* (E791 Collab.), Phys. Rev. D 57 (1998) 13.

[4] J. M. Link *et al.* (FOCUS Collab.), Phys. Lett. B 618 (2005) 23.

[5] B. Aubert *et al.* (Babar Collab.), Phys. Rev. Lett. 98 (2007) 211802.

[6] M. Staric *et al.* (Belle Collab.), Phys. Rev. Lett. 98 (2007) 211803.

[7] T. Aaltonen *et al.* (CDF Collab.), Phys. Rev. Lett. 100, 121802 (2008).

[8] I. Abt *et al.* (*HERA-B* Collab.), Eur. Phys. Jour. C 52 (2007) 531.

[9] C. Amsler *et al.* (Particle Data Group), Phys. Lett. B 667 (2008) 1.

[10] L. Zhang *et al.* (Belle Collab.), Phys. Rev. Lett. 96 (2006) 151801.

[11] `http://superb.kek.jp/`.

[12] `http://www.pi.infn.it/SuperB/`.

[13] P. Spradlin, G. Wilkinson, F. Xing *et al.*, LHCb public note LHCb-2007-049 (2007).

[14] `http://www.slac.stanford.edu/xorg/ hfag/charm/FPCP08/results_mix+cpv.html`.

[15] E. Barbierio *et al.* (Heavy Flavor Averaging Group), arXiv:0808.1297.

[16] S. E. Csorna *et al.* (CLEO Collab.), Phys. Rev. D **65**, 092001 (2002);

[17] B. Aubert *et al.* (BaBar Collab.), Phys. Rev. Lett. **100**, 061803 (2008).

[18] D. Acosta *et al.* (CDF Collab.), Phys. Rev. Lett. **94**, 122001 (2005).

[19] J. M. Link *et al.* (FOCUS Collab.), Phys. Lett. B **491**, 232 (2000); Err., Phys. Lett. B **495**, 443 (2000).

[20] E. M. Aitala *et al.* (E791 Collab.), Phys. Lett. B **421**, 405 (1998).

[21] J. E. Bartelt *et al.* (CLEO Collab.), Phys. Rev. D **52**, 4860 (1995).

[22] P. L. Frabetti *et al.* (E687 Collab.), Phys. Rev. D **50**, 2953 (1994).

[23] G. Bonvicini *et al.* (CLEO Collab.), Phys. Rev. D **63**, 071101 (2001).

[24] B. Aubert *et al.* (BaBar Collab.), arXiv:0802.4035 (2008).

[25] K. Arinstein *et al.* (Belle Collab.), Phys. Lett. B **662**, 102 (2008).

[26] D. Cronin-Hennessy *et al.* (CLEO Collab.), Phys. Rev. D **72**, 031102 (2005).

[27] S. Dobbs *et al.* (CLEOc Collab.), Phys. Rev. D **76**, 112001 (2007).

[28] S. Kopp *et al.* (CLEO Collab.), Phys. Rev. D **63**, 092001 (2001).

[29] X. C. Tian *et al.* (Belle Collab.), Phys. Rev. Lett. **95**, 231801 (2005).

[30] G. Brandenburg *et al.* (CLEO Collab.), Phys. Rev. Lett. **87**, 071802 (2001).

[31] D. M. Asner *et al.* (CLEO Collab.), Phys. Rev. D **70**, 091101 (2004).

[32] J. M. Link *et al.* (FOCUS Collab.), Phys. Lett. B **622**, 239 (2005).

[33] J. M. Link *et al.* (FOCUS Collab.), Phys. Rev. Lett. **88**, 041602 (2002); Err., Phys. Rev. Lett. **88**, 159903 (2002).

[34] E. M. Aitala *et al.* (E791 Collab.), Phys. Lett. B **403**, 377 (1997).

[35] B. Aubert *et al.* (BaBar Collab.), Phys. Rev. D **71**, 091101 (2005).

[36] G. J. Gounaris and J. J. Sakurai, Phys. Rev. Lett. 21: 244, 1968.

[37] B.-S. Zou, hep-ph/9611235.

[38] E.P. Wigner, Phys. Rev. 70, 15 (1946).

[39] E.P. Wigner and L. Eisenbud, Phys. Rev. 72, 29 (1947).

[40] I. J. R. Aitchison, Nucl. Phys. A189: 417-423, 1972.

[41] S. Kopp *et al.*, Phys. Rev. D63, 092001 (2001).

[42] "Dalitz Analysis of of $D^0 \to K^0_S\pi^+\pi^-$ and Measurement of the CKM Angle γ in $B^\pm$ Decays to $D^*K^\pm$ Decays", Ph. D. thesis by Y. P. Lau, SLAC-R-872.

[43] "Theoretical Nuclear Physics" by J. M. Blatt and V. F. Weisskopf, Dover Publications (1991).

[44] H. Pilkuhn, Relativistic Particle Physics, Springer, New York, 1979.

[45] "Hyperon and Hyperon Resonance Properties from Charm Baryon Decays at BaBar" by Veronique Ziegler (Univ. of Iowa). SLAC-R-868, May 2007.

[46] C. Amsler *et al.*, Physics Letters B667, 1 (2008): "Note on Scalar Mesons" by S. Spanier, N.A. Tornqvist and C. Amsler.

[47] C. Amsler *et al.*, Physics Letters B667, 1 (2008): "The $\eta(1405)$, $\eta(1475)$, $f_1(1420)$, and $f_1(1510)$ (Rev.)" by C. Amsler and A. Masoni.

[48] J. Adelman *et al.* (CDF Collab.), *The Silicon Vertex Trigger Upgrade at CDF*, Nucl. Instrum. Meth. A572, 361 (2007).

[49] M. L. Perl *et al.*, Phys. Rev. Lett. **35**, 1489 (1975).

[50] K. Kodama *et al.*, Phys. Rev. D **78**, 052002 (2008).

[51] K. Kodama *et al.* [DONUT Collaboration], Phys. Lett. B **504**, 218 (2001) [arXiv:hep-ex/0012035].

[52] R. Schwienhorst *et al.* [DONUT Collaboration], Phys. Lett. B **513**, 23 (2001) [arXiv:hep-ex/0102026].

[53] K. Abe *et al.* [Super-Kamiokande Collaboration], Phys. Rev. Lett. **97**, 171801 (2006) [arXiv:hep-ex/0607059].

[54] S. Fukuda *et al.* [Super-Kamiokande Collaboration], Phys. Rev. Lett. **85**, 3999 (2000) [arXiv:hep-ex/0009001].

[55] ArgoNeuT homepage: http://t962.fnal.gov.

[56] MicroBooNE collaboration, "A Proposal for a New Experiment Using the Booster and NuMI Neutrino Beamlines: MicroBooNE," 2007.

[57] S. Amerio *et al.* [ICARUS Collaboration], Nucl. Instrum. Meth. A **527**, 329 (2004).

[58] DUSEL homepage: http://www.lbl.gov/nsd/homestake.

[59] C. Amsler *et al.* [Particle Data Group], Phys. Lett. B **667**, 1 (2008).

[60] Y. Itow *et al.* [The T2K Collaboration], arXiv:hep-ex/0106019.

[61] A. Badertscher, M. Laffranchi, A. Meregaglia and A. Rubbia, New J. Phys. **7**, 63 (2005) [arXiv:physics/0412080]; A. Badertscher, M. Laffranchi, A. Meregaglia, A. Muller and A. Rubbia, Nucl. Instrum. Meth. A **555**, 294 (2005) [arXiv:physics/0505151]; A. Ereditato and A. Rubbia, Nucl. Phys. Proc. Suppl. **155**, 233 (2006) [arXiv:hep-ph/0510131].

[62] P. Astier *et al.* [NOMAD Collaboration], Nucl. Phys. B **611**, 3 (2001) [arXiv:hep-ex/0106102].

[63] S. Davidson, C. Pena-Garay, N. Rius and A. Santamaria, JHEP **0303**, 011 (2003) [arXiv:hep-ph/0302093].

[64] A. Friedland and C. Lunardini, Phys. Rev. D **72**, 053009 (2005) [arXiv:hep-ph/0506143].

[65] M. Hirsch, E. Nardi and D. Restrepo, Phys. Rev. D **67**, 033005 (2003) [arXiv:hep-ph/0210137].

[66] G. 't Hooft, Phys. Lett. B **37**, 195 (1971).

[67] T. Adams *et al.* [NuSOnG Collaboration], arXiv:0803.0354 [hep-ph].

[68] T.Asaka and M. Shaposhnikov, Phys.Letters B620 (2005) 17; M. Shaposhnikov, Nucl.Physics B 763 (2007)49; M. Shaposhnikov, astro-ph/0703673; A.D.Dolgov et al., astro-ph/0008138, M.Viel et al., astro-ph/0501562

[69] G.Bernardi et al, Phys.Letters 166B (1986) 479 G.Bernardi et al, Phys.Letters B203 (1988) 332 P.Astier et al., Phys.Letters B506 (2001) 27